Top-Down Projections of the Prefrontal Cortex to the Ventral Tegmental Area, Laterodorsal Tegmental Nucleus, and Median Raphe Nucleus

Rudieri Souza
Institute of Biomedical Sciences, University of São Paulo
Debora Bueno
Institute of Biomedical Science, University of São Paulo
Leandro B. Lima
Institute of Biomedical Sciences, University of São Paulo
Luciano Gonçalves
Universidade Federal do Triângulo Mineiro Faculdade de Medicina: Universidade Federal do Triangulo Mineiro Faculdade de Medicina
Jose Donato Jr.
Institute of Biomedical Sciences, University of São Paulo
Sara J. Shammah-Lagnado
Institute of Biomedical Sciences, University of São Paulo
Martin Metzger (metzger@icb.usp.br)
Institute of Biomedical Sciences, University of São Paulo https://orcid.org/0000-0002-3155-9814

Research Article

Keywords: prefrontal cortex, top-down control, dopamine, serotonin, acetylcholine

Posted Date: October 20th, 2021

DOI: https://doi.org/10.21203/rs.3.rs-979767/v1

Top-down projections of the prefrontal cortex to the ventral tegmental area, laterodorsal tegmental nucleus, and median raphe nucleus

Rudieri Souza[1#], Debora Bueno[1], Leandro B. Lima[1], Luciano Gonçalves[2], Jose Donato Jr[1], Sara J. Shammah-Lagnado[1], Martin Metzger[1*],

[1]Department of Physiology & Biophysics, Institute of Biomedical Sciences, University of São Paulo, 05508-900 São Paulo, Brazil, [2]Department of Human Anatomy, Federal University of the Triângulo Mineiro, 38025-180 Uberaba, Brazil

Rudieri Souza ORCID 0000-0001-7404-5605

Jose Donato Jr. ORCID 0000-0002-4166-7608

Martin Metzger ORCID 0000-0002-3155-9814

Keywords: prefrontal cortex; top-down control; dopamine; serotonin; acetylcholine

***Corresponding author:** Martin Metzger, PhD

Dept. of Physiology & Biophysics, Institute of Biomedical Sciences I

University of São Paulo, USP

Av. Prof. Lineu Prestes 1524

05508-900 São Paulo, SP, Brazil

Phone: 55/11/30917255; Fax: 55/11/30917285

E-mail address: metzger@icb.usp.br

Abstract: Anatomical and functional evidence suggests that the PFC is fairly unique among all cortical regions, as it not only receives input from, but also robustly projects back to mesopontine monoaminergic and cholinergic cell groups. Thus the PFC is in a position to exert a powerful top-down control over several state setting modulatory transmitter systems that are critically involved in the domains of arousal, motivation, reward/aversion, working memory, mood regulation, and stress processing. Regarding this scenario, the origin of cortical afferents to the ventral tegmental area (VTA), laterodorsal tegmental nucleus (LDTg), and median raphe nucleus (MnR) was here compared, by using the retrograde tracer cholera toxin subunit b (CTb). CTb injections into VTA, LDTg, or MnR produced retrograde labeling in the cortical mantle, which was mostly confined to medial, orbital, and lateral PFC subdivisions, along with rostral and mid-cingulate areas. Remarkably, in all of the three groups, retrograde labeling was densest in layer V pyramidal neurons of the infralimbic, prelimbic, medial orbital and frontal polar cortex. Moreover, a conspicuous lambda-shaped region around the apex of the rostral pole of the nucleus accumbens stood consistently out as heavily labeled. At almost all rostrocaudal levels through the PFC analyzed, retrograde labeling was strongest following injections into MnR and weakest following injections into VTA. Altogether, our findings reveal a broadly similar set of prefrontal afferents to VTA, LDTg, and MnR, further supporting an eminent functional role of the PFC as a controller of all major state setting mesopontine modulatory transmitter systems.

Introduction

The rodent prefrontal cortex (PFC) is a group of tightly interconnected brain regions located over the medial, orbital, and insular surfaces of the rostral pole of the cerebral hemispheres (Gabbott et al. 2005; Heidbreder and Groenewgen 2003; Hoover and Vertes 2007; Murphy and Deutch 2018; Van Eden and Uylings 1985). As a whole, the PFC is situated at the apex of the perception-action cycle in the brain (Fuster 2001). It supports higher executive functions (Euston et al. 2012; Miller and Cohen 2001), such as impulse control, behavioral flexibility, reversal learning (Rich and Shapiro 2007, 2009; Ragozzino et al. 1999), working memory (Sawaguchi and Goldman-Rakic 1994), and decision making (Bechara and Damasio 2005), necessary to organize behavior in time and context (Kolb et al. 2012). Although, the structural homology of the rodent and primate PFC is still a matter of debate (e.g. Carlén 2017), findings from lesion studies support that distinct parts of the rodent PFC fulfill similar executive functions than in primates (for review, see Dailey et al. 2004; Kesner and Churchwell 2011; Ragozzino 2007). Some cell type specific circuits and transcriptomics have recently been described in the rodent PFC (Ährlund-Richter et al. 2019; Anastasiades and Carter 2021; Dembrow and Johnston 2014; Tasic et al, 2018). However, except of the lack of layer IV (Van de Werd and Uylings 2008; Van de Werd et al. 2010; Van Eden and Uylings 1985), the overall circuit organization of the agranular rodent PFC is fairly similar to neocortical areas (Harris and Shepherd 2015). Hence, it has been advocated that what differentiates the PFC from other cortical areas and underlies its memory and executive functions is rather its characteristic set of mostly reciprocal connections with higher order sensory/motor areas, the hippocampal formation, and state setting modulatory transmitter systems. Moreover, this specific connectivity enables the PFC to deal with different types of memory (Euston et al. 2012; Tulving and Schacter 1994) and exert a

top-down control of behavior (Artigas 2010; Miller and Cohen 2001). Regarding these modulatory transmitter systems, just like all cortical areas, the PFC receives broad serotonergic and non-serotonergic innervation from the dorsal (DR) and median (MnR) raphe nucleus (Bang and Commons 2012; Muzerelle et al. 2016; Ren et al. 2019; Szönyi et al. 2016; Vertes et al. 1999; Vertes, 1991), as well as noradrenaline (NA)-only inputs from the locus coeruleus (LC; Chandler et al. 2019; Loughlin et al. 1982; Schwarz and Luo 2015). In addition, the rodent PFC is the principal cortical target of a dopamine (DA)-only or multiplexed DA/GABA/glutamate (GLU) innervation (Barker et al. 2016; Kalsbeek et al. 1988; Lindvall et al. 1974; Taylor et al. 2014), primarily arising from the ventral tegmental area (VTA; for review, see Björklund and Dunnett 2007; Deutch 1993; Morales and Margolis 2017). Cholinergic inputs to PFC emerge from the basal forebrain (Saper 1984; Woolf and Butcher 2011) and also from the mesopontine laterodorsal tegmental nucleus (LDTg; Satoh and Fibiger 1986).

Notably, differentially from most other cortical regions, the PFC not only receives input from, but also robustly projects back to all major mesopontine monoaminergic and cholinergic cell groups (Bueno et al. 2019; Gabbott et al. 2005; Heidbreder and Groenewegen 2003; Luppi et al. 1995; Ogawa et al. 2014; Sesack et al. 1989). Thus, specific PFC subareas can exert a top-down control over ascending monoamine systems by means of descending projections to the nuclei of origin (Phillips et al. 2008; Robbins 2005). Among all monoaminergic cell groups, prefrontal inputs to the DR have been explored in greatest detail (Pollak Dorocic et al. 2014; Gonçalves et al. 2009; Jankowski and Sesack 2004; Peyron et al. 1998; Weissbourd et al. 2014). Neuronal activity in the DR can be powerfully regulated by prefrontal inputs (Celada et al. 2001; Hajós et al. 1998), a mechanism, now shown to be involved in mood regulation (Challis et al 2014; Geddes et al 2016), response to stress (Amat et al. 2005, 2008; Soiza-Reilly et al. 2019;

Warden et al. 2012), and in the actions of antipsychotic (Artigas 2010) and hallucinogenic drugs (Martin-Ruiz et al. 2001; Gonzalez-Maeso et al. 2007).

Interestingly, the PFC is one of few cortical regions, reciprocally interconnected to both DR and MnR (Hoover and Vertes 2007; Pollak Dorocic et al. 2014; Vertes 1991; Vertes et al. 1999). Findings from pharmacological and optogenetic studies now point to a major role of MnR circuits in depression (Graeff et al. 1996; Teissier et al. 2015; Szönyi et al. 2019) and anxiety (Abela et al. 2020; Andrade et al. 2013; Ohmura et al. 2014, 2020). Similar to MnR (Behzadi et al. 1990), it is well acknowledged that the PFC, mostly by means of glutamatergic pyramidal cells, monosynaptically projects back to the VTA (Geisler and Zahm 2005, 2006; Geisler et al. 2007; Phillipson 1979; Sesack and Pickel 1992; Watabe-Uchida et al. 2012). Electrical stimulation of the medial PFC (mPFC) either excites or inhibits VTA neurons (Overton et al. 1996; Overton 1997; Tong et al. 1996, 1998). Interestingly, the top-down modulation exerted by the PFC occurs in a sub-region/circuit specific manner. Thus, whereas single-pulse stimulation in the mPFC mostly excites putative VTA DA neurons, stimulation of the orbital PFC (oPFC) mostly inhibits them (Lodge 2011). Furthermore, as clarified in an elegant electron-microscopic study, PFC axons preferentially contact VTA DA neurons that project back to the mPFC (Carr and Sesack 2000). Given that individual mPFC cells can send collaterals to both, VTA and DR (Vázquez-Borsetti et al. 2011), this implies that PFC is able to adjust its own DA input from VTA, and also simultaneously impact other brainstem modulatory cell groups (Dembrow and Johnston 2014).

The LDTg is a major cholinergic cell group localized in the periventricular mesopontine tegmentum (Mesulam et al. 1983). LDTg is considered a key component of the ascending reticular activating system (Steriade et al. 1990) and a master regulator of the firing pattern of VTA DA neurons (Dautan et al. 2016; Lodge and Grace 2006).

We recently reexamined the neuronal connections of the LDTg, highlighting that LDTg receives ample inputs from mPFC, lateral habenula (LHb), and lateral hypothalamus. This characteristic connectivity pattern might put LDTg on a similar level as an authentic ascending state-setting modulatory system like VTA, DR, and MnR (Bueno et al. 2019). However, in contrast to the DR (Gonçalves et al. 2009; Peyron et al. 1998), a detailed investigation of the areal and laminar origin of prefrontal afferents to MnR and LDTg is to our best knowledge still lacking. For the VTA, such an analysis was performed in the seminal study of Gabbott et al. (2005). However, in this study, the VTA was only one of several subcortical PFC targets investigated, and the complex cellular/connectional heterogeneity of distinct VTA compartments (Barrot 2014; Breton et al. 2019; Lammel et al. 2011, 2012; 2014; Morales and Margolis 2017; Verharen et al. 2020) was not considered. Thus, in the present study the origin of prefrontal afferents to different parts of the VTA, as well as to the LDTg and MnR was investigated in a comparative manner in rats by using cholera toxin subunit b (CTb) as retrograde tracer.

Materials and methods

Animals and surgery

Adult male (n = 10) and female (n = 2) Wistar rats (160-220 g), fed ad libitum and kept under controlled environmental conditions (12h light/dark cycle, light on at 7:00 A.M.; room temperature 22 °C) were used in our analysis. These cases make part of a much larger in-house set of animals (more than 80) with retrograde tracer injections into the VTA, LDTg, or MnR. All the procedures were approved by the ethical committee of animal experimentation of the Institute of Biomedical Sciences of the University of São Paulo and were in accordance with the NIH Guidelines for the Use and Care of Laboratory Animals.

The rats were anesthetized with a mixture of 10 mg/kg of xylazine (i.p.; Vetbrands, São Paulo, Brazil) and 90 mg/kg of ketamine (i.p., Vetbrands, São Paulo, Brazil) and iontophoretic injections of cholera toxin subunit b (1% of low salt CTb in distilled water; List Biological Lab, Campell, CA) were made in VTA, LDTg, or MnR. The tracer was delivered through a glass micropipette (internal tip diameter 15-20 µm) by using a positive-pulsed (7 seconds on, 7 seconds off) current set at 5.0 µA for 15-20 minutes. The stereotaxic coordinates were extracted from the rat brain atlas of Paxinos and Watson (2007) and refined empirically subsequently: VTA: AP = -5.2 to -6.0 mm caudal to the bregma; ML = 0.0 to 0.9 mm from the midline; DV = -8.0 to -8.6 mm below the dura. LDTg: AP = -8.5 to -8.8 mm caudal to the bregma; ML = 0.6 to 0.8 mm from the midline; DV = -6.4 to -6.6 mm below the dura. MnR: AP = -7.8 to -8.4 mm caudal to the bregma; ML = 0.0 mm from the midline; DV = -8.2 to -8.5 mm below the dura. Before withdrawal, the pipette was left in situ for 5 minutes, and a negative current, set at 2µA, was applied to minimize tracer backflow along the pipette tract.

Perfusion and tissue processing

After 7 days, the animals were deeply anesthetized and perfused transcardially with 90 ml of 0.9% saline followed by 500 ml 4% paraformaldehyde in 0.1 M phosphate buffer (PB; pH 7.3) at 4ºC. The brains were post-fixed for 4 hours at 4ºC and then cryoprotected overnight with 20% sucrose solution in PB at 4ºC. Brains were sectioned in the coronal plane at 40 µm into four series on a sliding microtome (Model 2010R, Leica, Nussloch, Germany). One or two series of sections were processed for CTb immunohistochemistry (Luppi et al. 1990). An adjacent series was stained with thionin for cytoarchitectonic analysis. Another series was used for double- or triple imunoflurescence staining experiments in order to better delineate labeled structures and injection target areas.

Antibody characterization and immunohistochemical controls

The primary antibodies used in this study (Table 1) have been fully characterized and tested for specificity. The goat antibody against **CTb** (List, #104, RRID: AB_2313636) was raised against the purified toxin from Vibrio cholerae (List datasheet), which is not physiologically present in the organism. The rabbit antibody against **serotonin** (5-HT; Immunostar, Hudson, WI, #200800, RRID: AB_572263) was raised against 5-HT derived from rat brain, coupled to bovine serum albumin (BSA) with paraformaldehyde. The mouse antibody against neurofilament H (**SMI-32**; Biolegend, San Diego, CA, #801701, RRID: AB_2564642) was raised against non-phosphorylated mammalian neurofilament H (Sternberger and Sternberger, 1983). This antibody stains a subpopulation of pyramidal cells and is well suited to recognize their apical dendrite orientation, as well as to detect areal boundaries (e.g. Van De Weerd and Uylings, 2008). The rabbit monoclonal antibody against the neuronal nuclear protein marker (**NeuN**; Abcam, Cambridge, UK, #177487, RRID: AB_2532109) was raised against a synthetic peptide of unspecified length chosen from within the residues 1–100 of human NeuN.

Optimal antibody concentrations were individually determined for each antibody. Specificity of the secondary antibodies was indicated by the observed absence of labeling in tissue sections collected from naive animals and animals that had received a tracer injection, to which the immunohistochemical method was applied with omission of the primary antibody step.

Single immunoperoxidase labeling protocol for CTb

Sections were preincubated for 30 minutes in 2% normal donkey serum (NDS, Jackson Immunoresearch Laboratories, West Grove, PA) and then incubated with a polyclonal anti-CTb raised in goat (List) diluted 1:10.000 in PB containing 0.3% Triton X-100 for

48 hours at 4°C. Sections were subsequently rinsed in PB and incubated for 2 hours at room temperature in biotinylated donkey anti-goat secondary antibodies (Jackson Immunoresearch) diluted 1:4.000 in PB. Sections were rinsed again followed by 2 hours incubation in an ABC Kit (ABC Elite Kit, Vector Laboratories, Burlingame, CA). After thorough rinsing in PB, the peroxidase reaction product was visualized using the glucose oxidase procedure (Itoh et al. 1979) and the metal-free 3,3'-diamenobenzidine (DAB) tetrahydrochloride as chromogen. Sections were washed again extensively in PB, mounted on gelatinized slides, air dried, dehydrated, and coverslipped with DPX.

Multiple immunofluorescence labeling protocols

In order to better judge the exact position of CTb labeling in the PFC, selected sections from rats with CTb injections into the LDTg were submitted to immunofluorescence triple-labeling for NeuN/SMI-32/CTb. Moreover, in order to better estimate the size and extent of CTb injections into the MnR, selected sections through the mesopontine tegmentum from rats with prior tracer injections into MnR were submitted to immunofluorescence double-labeling for 5-HT/CTb. For these purposes sections were preincubated for 30 minutes in 2% normal donkey serum (NDS, Jackson Immunoresearch). Sections were then incubated for 48 hours at 4°C in a cocktail of 3 or 2 primary antibodies containing either (a) rabbit anti-NeuN, 1:2.500/mouse anti-SMI-32, 1:2.500/goat anti-CTb, 1:10.000 or (b) rabbit anti-5-HT, 1:40.000/goat anti-CTb, 1:10.000, respectively. All primary antibodies were diluted in PB containing 1% normal donkey serum (NDS, Jackson) and 0.3% Triton X-100. Sections were subsequently rinsed in PB and incubated for 1 hour in cocktails of 3 or 2 secondary antibodies consisting of either (a) Alexa488-conjugated donkey anti-mouse/Alexa594-conjugated donkey anti-goat/Alexa647-conjugated donkey anti-rabbit, or (b) Alexa488-conjugated donkey anti-rabbit/Alexa594-coinjugated donkey anti-goat (all from Jackson

Immunoresearch, diluted 1:500 in PB containing 1% NDS), respectively. Sections were finally thoroughly rinsed in 0.05 M Tris-HCl, mounted on gelatine-coated slides, coverslipped with slow-fade-medium (Invitrogen, Carlsbad, CA), and sealed with nail polish.

Several sets of controls were performed, including the omission of one, two, or three primary antibodies, omission of one, two, or three of the secondary antibodies, and switching of the fluorophores related to the different markers. All these control procedures resulted in the expected single or double fluorescence labeling or, in the case of omission of all primary antisera, in the absence of fluorescence labeling.

Data analysis and quantification of CTb-labeled neurons

The immunostained sections were examined under bright- and darkfield microscopy using a Zeiss Axioimager A1 microscope (Zeiss, München, Germany). Digital color photomicrographs were acquired using a Zeiss Axiocam 512 colour camera (Zeiss). Selected double- or triple- immunofluorescence stained sections were analyzed with a Zeiss LSM 780 confocal laser scanning microscope (Zeiss, Goettingen, Germany) using step intervals of about 200 nm along the z-axis. Quantification of CTb positive (CTb+) cells was performed on images of whole ipsilateral hemisphere. Such images were typically captured from six standardized coronal sections per animal, representing levels spanning from about 5.3 mm to 2.3 mm anterior to Bregma along the rostrocaudal axis of the pregenual PFC. For this purpose, depending on the size of the hemisphere, 4 to 9 photomicrographs were taken with a Zeiss 5x/0.16 objective. Photomontages were arranged using the Adobe Photoshop software (Version 7.0; Adobe Systems Inc., Mountain View, CA). Since the selection of the six analyzed PFC sections was based on the presence of characteristic morphological landmarks, they were not spaced uniformly. However, all analyzed sections were at least 160 µm apart from one another.

Drawings of the selected PFC sections and electronic plotting of all retrogradely labeled cells within them were performed on brightfield and inverted brightfield photomicrographs uploaded to the computer drawing program Canvas X, Version 20 (ACD Systems, Victoria, Canada). CTb+ cells were electronically counted within 11 PFC subregions of the ipsilateral hemisphere in 12 cases with injections largely restricted to the VTA (n = 6), LDTg (n = 3), or MnR (n = 3). The numbers of labeled cells were first converted to densities by dividing counted cells by the area of the prefrontal region selected for counting. Then, the relative densities were scaled to the maximum value within that brain. A similar semi-quantitative analysis was previously used by Floyd et al. (2000) and Gonçalves et al. (2009). In the above described cases/regions, we then compared the absolute numbers of retrogradely labeled cells in the six analyzed PFC sections along the rostrocaudal axis. Quantification of CTb+ neurons in the contralateral hemisphere was performed in only one of the standard PFC levels (level 4 at about 2.8 mm anterior to Bregma) and was restricted to anterior cingulate area 1 (Cg1), prelimbic (PrL), and infralimbic (IL) cortex. Image processing and lettering was carried out with Adobe Photoshop (Version 7.0). Color balance, contrast, and brightness of the images were adjusted to a variable extent. The Canvas X software (Version 20) was used for line drawings.

Statistical analysis: Data were analyzed by one-way ANOVA, followed by Newman-Keuls multiple comparisons test. Statistical analyses were performed using the GraphPad Prism software (version 8.02, San Diego, CA). We considered p values $\leq$ 0.05 to be statistically significant. All results are expressed as mean ± SEM.

Nomenclature: The nomenclature used in the present study is based on the atlas of Paxinos and Watson (2007) unless otherwise specified. In general terms, according to Heidbreder and Groenewegen (2003), we divided the PFC into mPFC, oPFC and lateral

PFC (lPFC), and additionally distinguished a frontal polar (FP) region, which according to Ray and Price (1992) was subdivided into a separate medial (FPm) and lateral (FPl) frontal polar area. Noteworthy, the term oPFC refers here to the medial (MO), ventral (VO), and lateral (LO) areas of the orbitofrontal cortex (Groenewegen 1988), whereas lPFC includes the ventral (AIV) and dorsal (AID) parts of the agranular insular cortex. We also included the rostral secondary motor cortex (M2) into our analysis. In rats, the rostral part of M2, formerly termed medial agranular (AGm) or precentral medial cortex (PrCm), receives robust inputs from the lateral segment of the mediodorsal nucleus of the thalamus (Ray and Price 1992; Hoover and Vertes 2007). Thus, along with Cg1, PrL, and IL districts, the rostral part of M2 is traditionally considered an integral component of the rodent mPFC (Krettek and Price 1977). In the nucleus accumbens, we distinguished a separate rostral pole area (AcbRP) as proposed by Zahm and Heimer (1993). Finally, we here also differentiate a hitherto ill-defined presumptive non-cortical region intertwined between the IL/dorsal peduncular (DP) and the VO cortical areas. This histologically cell-poor region sits astride the apex of the AcbR/ependym of the olfactory ventricle (EOV; Figs. 3a, b) and was consistently filled by CTb+ neurons following our tracer injections into either, VTA, LDTg, or MnR. Due to its characteristic shape, most evident in coronal sections at levels about 2.8 mm rostral to Bregma, we here tentatively named it area Lambda (λ). Importantly, a pattern of clustered retrograde labeling occupying area λ has already been perceived in previous tracing studies, exploring prefrontal afferents to the DR (Gonçalves et al. 2009), VTA (Geisler and Zahm 2005, 2006; Yetnikoff et al. 2015), or LDTg (Bueno et al. 2019).

Results

Tracer injections

Representative examples of most CTb injections into the VTA, LDTg, and MnR, analyzed in the present study, are illustrated in Figure 1. All our CTb injections into the VTA (Fig. 1 a–f) were largely confined to the VTA and typically involved the rostral and middle two-thirds of this structure. Cases in which the injection encroached onto the caudally adjacent rostromedial tegmental nucleus (RMTg) or medially adjacent interpeduncular nucleus (IP) were excluded from analysis. This criterion was rigorously applied, since both, RMTg (Yetnikoff et al. 2015) and IP (Lima et al. 2017) receive substantial PFC input. Three of our VTA injections (cases R30, R694, R696) were centered in the dorsolateral VTA, they were relatively large and mostly occupied the parabrachial pigmented subnucleus (PBP) and, except of case R30, also the adjacent paranigral (PN) subnucleus in their entire extent along the rostrocaudal axis (Fig. 1a-c). In case R694, the injection slightly impinged on the compact part of the substantia nigra (SNC). The injections in cases R70, R 620, and R621 were placed in the ventromedial VTA. Thus, they were centered on the PN (case R70; Fig. 1d), or the midline interfascicular (IF) and rostral linear (RLI) subnuclei of the VTA (cases 620, 621, Fig. 1e, f).

CTb injections into LDTg (n = 3) were typically centered within the middle one-third along its rostrocaudal axis at about 8.6 mm posterior to Bregma (Fig. 1g, h; inset in Fig. 7a). Beside minimal encroachment on the medially adjacent pericentral part of the dorsal tegmental nucleus (DTgP), all the three CTb injections into LDTg were largely restricted to this nucleus and typically filled its dorsal part.

CTb injections into MnR (n = 3) were centered on its middle and caudal two-thirds (Fig. 1 i–k). They occupied the MnR core to a different degree and also involved the

adjoining paramedian raphe nucleus (PMnR). Moreover, in two of these cases (RD80, RD81) our injections peripherally encroached on the interstitial part of the dorsal raphe nucleus (DRI), without substantially affecting the DR proper.

Relative densities of prefrontal afferents to VTA

Following CTb injections in different VTA districts, all subregions of the FP, mPFC, oPFC, and lPFC analyzed contained CTb+ neurons (Fig. 2a). Some characteristic features of the resulting retrograde labeling in the PFC are depicted in Figure 3, and the distribution pattern of retrograde labeling charted in 3 cases (R30, R694, R620) is illustrated in Figures 4–6. In general, most of the CTb+ neurons following tracer injections into VTA were classified as layer V pyramidal cells (72.53 ± 7.62%, n = 6, sample size = 2.704; Fig. 3a-c). About one quarter (27.64 ± 7.44%, n = 6, sample size = 924) of CTb+ neurons, composed chiefly of multiform cells, were located in layer VI. Pretty rarely we observed CTb+ neurons in layers II/III (0.40 ± 0.14%, n = 6, sample size = 16). CTb labeling in the PFC was predominantly ipsilateral. As evaluated for the three cases with injections into the dorsolateral VTA, CTb+ neurons in Cg1, PrL, and IL of the contralateral hemisphere accounted for about 17.83 ± 2.16% (n = 3, sample size = 153) of the CTb labeling found in equivalent areas of the ipsilateral hemisphere.

In the three cases with CTb injections aimed at the dorsolateral VTA, all mostly filling the PBP (R30, R694, R696), we found a highly consistent pattern of retrograde labeling. Thus, in the mPFC, the IL and PrL, along with FPm more rostrally, stood out as the most densely labeled subregions (Fig. 2a). Noteworthy, CTb+ neurons in the IL were particularly enriched in its caudal part (Figs. 4d-f). Compared to IL, PrL, and FPm, CTb labeling considerably thinned out in the two dorsal mPFC subregions, the Cg1 and M2, as well as in the FPl (Figs. 2, 4-6). Among the subregions of the oPFC, the MO invariably presented the highest density of CTb+ neurons, followed by the VO. A band

of CTb+ neurons typically stretched over the LO, AIV, and AID, which all presented comparably low densities of CTb+ neurons (Figs. 4, 5). Ventrally to IL, the dorsal peduncular cortex (DP) was densely labeled. However, apart from DP, cortical CTb labeling outside the PFC was generally meager, with some scattered CTb+ neurons occasionally found in the primary motor (M1) and somatosensory (S1) cortex, the dysgranular (DI), and granular (GI) insular cortex (Fig. 4), as well as more caudally in the cingulate area 2 (Fig. 11c). Only case R694, in which the CTb injection slightly encroached onto SNC, displayed substantial numbers of CTb+ neurons in M1, S1, DI, and GI (Fig. 5).

Compared to the cases with injections into PBP, CTb labeling was more heterogeneous and less dense in the remainder 3 cases, with injections restricted to the midline VTA subnuclei IF/CLI (cases R620, R621) or to PN. However, the general pattern and relative densities of CTb labeling in these cases little changed. Thus, in R620 (Fig. 6) and R621 the FPm and IL were again the most densely labeled PFC subregions. Moreover, in case R621 all oPFC and lPFC subregions displayed a relatively denser label than in other cases. In case R70, in which the injection was fairly confined to PN, FPm was only moderately labeled and the MO stood out as the most densely labeled PFC subregion.

In the PFC sections analyzed here, non-cortical CTb labeling following VTA injections was consistently found in the claustrum (Cl), nucleus accumbens shell (AcbSh), and ventral pallidum (VP); but was particularly prominent in an area tentatively named area λ (Figs. 3a, d, 4d, 5d). The CTb labeling in area λ consisted of densely clustered polymorph neurons (Fig. 3d) located astride both sides of the apex of the AcbRP/EOV and extending dorsally into the white matter that forms the forceps minor of the corpus callosum.

Relative densities of prefrontal afferents to LDTg

Following CTb injections into LDTg, all subregions of the FP, mPFC, oPFC, and lPFC contained CTb+ neurons (Fig. 2b). Some characteristic features of the resulting retrograde labeling in the PFC are illustrated in Figure 7, and its distribution, plotted in the representative case R67, is illustrated in Figure 8. Again, the vast majority of CTb+ neurons following LDTg injections were classified as layer V pyramidal cells (89.59 ± 2.53%; n = 3, sample size = 2.622; Fig. 7a). About one tenth of CTb+ neurons (10.72 ± 2.42%, n = 3, sample size = 315) were located in layer VI, most of them in IL and the ventral part of PrL. CTb labeling was predominantly ipsilateral. However, contralateral CTb+ neurons in the Cg1, PrL, and IL accounted for about half (49.22 ± 3.93%, n = 3, sample size = 374) of the CTb labeling present in the equivalent regions of the ipsilateral hemisphere (Fig. 7a).

Overall, the general pattern of CTb labeling in the three cases with LDTg injections was highly consistent (Fig. 2b). As described for the VTA, in the mPFC, the IL and PrL, along with FPm more rostrally, displayed the highest densities of CTb+ neurons (Fig. 2b, 8). A moderate to high density of CTb+ neurons was detected in the Cg1, whereas low densities were found in M2 and FPl. In the oPFC, MO and VO were more densely labeled than in cases with VTA injections, whereas LO, AIV, and AID displayed only low densities of CTb+ neurons (Fig. 2b). Except of prominent labeling in the DP, and moderate numbers of CTb+ neurons found more caudally in the Cg2, the remainder cortical mantle was almost devoid of CTb labeling following injections into LDTg. Non-cortical labeling in the here analyzed 6 prefrontal sections was modest in the Cl, AcbSh, and VP. However, area λ was again densely labeled (Figs. 7b-d, 8d). As revealed by counterstaining sections through area λ with the neuron marker NeuN and the neurofilament marker SMI-32, CTb labeling in area λ was distinct from that in

layers VI of DP and VO, between which most of area λ is interposed. Thus, the majority of the primarily oval to round CTb+ neurons in area λ were typically located amidst two streams of SMI-32+ axons astride the apex of the AcbRP, which dorsally gathered in direction of the forceps minor of the corpus callosum (Figs. 7b-d).

Relative densities of prefrontal afferents to MnR

CTb injections into MnR produced retrograde labeling in all analyzed subregions of the FP, mPFC, oPFC, and lPFC (Fig. 2c). Characteristic features of this labeling are illustrated in Figure 9, and the distribution pattern of CTb+ neurons plotted in our representative case R60 is illustrated in Figure 10. Again, the great majority (88.95 ± 0.40%, n = 3, sample size = 3.025) of CTb+ neurons were classified as layer V pyramidal cells (Figs. 10, 11). Little more than 10% (11.02 ± 0.40%, n = 3, sample size = 376) of the CTb+ cells were located in layer VI. Most of them were multiform cells located in IL and PrL. Since we used a midline approach to target MnR, the resulting retrograde labeling was essentially bilateral.

Different from cases with CTb injections into VTA, MO was the most densely labeled PFC region following MnR injections, with compact labeling also found in the adjacent VO (Fig. 2c). In the mPFC, the IL, PrL, and again more rostrally FPm (Fig. 9a), were most densely labeled, whereas relatively minor densities of CTb+ neurons were charted in FPl, M2, and Cg1. Again, the LO, AIV, and AID presented comparable low densities of retrogradely labeled neurons. Scattered cortical labeling outside the PFC was mainly found in the DP, M1, frontal area 3, and S1. Noteworthy, CTb injections into MnR produced considerable more robust labeling throughout the mid-cingulate areas 1 and 2 (24a' and 24b' of Vogt and Paxinos 2014) compared to those observed following injections into VTA or LDTg (Fig. 11). Few CTb+ neurons were also consistently found more caudally in the retrosplenial dysgranular cortex. Non-

cortical labeling in the here analyzed 6 prefrontal sections was observed in the Cl, AcbSh, and VP (Fig. 10d-f). Finally, area λ was again densely labeled.

Absolute numbers of retrogradely labeled cells along the rostrocaudal axis

Mainly to compare the distribution of VTA-, LDTg- and MnR- projecting neurons along the rostrocaudal axis of the PFC, we also evaluated the absolute numbers of retrogradely labeled neurons in the three groups with CTb injections into VTA, LDTg, or MnR. Importantly, considering that tracer uptake depends on several factors including the shape and size of the injected structure, normally resulting in incomplete coverage of the target region, strong conclusions from differences in absolute counts between projection targets should be avoided (Breton et al. 2019). Nevertheless we observed some tendencies in our material. Thus, for any of the six rostrocaudal PFC levels analyzed, the greatest numbers of CTb+ neurons were consistently found in cases with MnR injections (Fig. 12). This difference became statistically significant in level 2, 5, and 6. Except for the rostralmost (FP) level, cases with LDTg injections presented higher absolute numbers in all herein analyzed rostrocaudal levels through the pregenual PFC, as compared to PFC. However, this difference became statistically relevant only in the caudalmost PFC level (level 6).

DISCUSSION

In the present study, we explored by retrograde tracing prefrontal top-down projections to three state setting neuromodulatory cell groups, the VTA, LDTg, and MnR. We disclosed 1) that these three mesopontine structures receive a rich and fairly similar set of prefrontal afferents, mainly emerging from ventromedial PFC subregions including the IL, PL, MO, VO, and FPm (see Summary Diagram in Fig. 13); 2) our findings strongly reinforce the view that PFC is the principal source of cortical afferents to the

VTA, LDTg, and MnR, with some additional cortical inputs arising from PFC-related cortices such as DP and cingulate areas; and 3) we also spotlight a hitherto little-specified cell-poor region astride the AcbRP as a major afferent source of VTA, LDTg, and MnR. Our findings will be discussed with reference to earlier studies examining prefrontal inputs to monoaminergic and cholinergic cell groups, as well as to the functional role of prefrontal top-down projections to state setting neuromodulatory systems in normal behavior and psychiatric disease.

Comparison with previous studies on prefrontal inputs to VTA, LDTg, and MnR

Overall, the major part of our findings is in good agreement with the results of earlier conventional tracing studies addressing prefrontal afferents to the VTA (Gabbott et al. 2005; Geisler and Zahm 2005; Geisler et al. 2007; Phillipson 1979), LDTg (Bueno et al. 2019; Cornwall et al. 1990; Satoh and Fibiger 1986; Semba and Fibiger 1992), and MnR (Behzadi et al. 1990). Having in mind that some of these previous studies used retrograde tracers far less sensitive than CTb (Luppi et al. 1990), only major correlations and discrepancies with their findings will be addressed here. Interestingly, our results are occasionally at odds with those from recent viral tracing studies investigating monosynaptic inputs to distinct cell groups in the VTA (Beier et al. 2015, 2019; Watabe-Uchida et al. 2012; Ogawa et al. 2014), LDTg (Wang et al. 2019) or DR/MnR (Pollak-Dorocic et al. 2014) with modified rabies virus (Wickersham et al. 2007). These discrepancies will be broadly debated.

Regarding the VTA, our findings are well in line with those of earlier conventional retrograde tracing studies from Zahm and co-workers (Geisler and Zahm 2005, 2006; Yetnikoff et al. 2015). Thus, as described in their material, ventral subdivisions of the mPFC such as IL and PrL were among the most densely labeled regions in our study, whereas agranular insular areas in the lPFC appeared weakly labeled. Moreover, there is

now abundant evidence indicating that the bulk of PFC inputs to the VTA and other mesopontine structures such as the DR, MnR, and LDTg arises from glutamatergic layer V pyramidal neurons (Spruston 2008), with some additional inputs coming from multiform cells in layer VI (present findings, Gabbott et al. 2005; Geisler et al. 2007; Vázquez-Borsetti et al. 2009). Regarding, the only recently fully recognized cellular and functional heterogeneity of the VTA (e.g. Lammel et al. 2008; Morales and Margolis 2017; Sanchez-Catalan et al. 2014), our findings indicate that dorsolateral and ventromedial subdivisions of the VTA, with some quantitative differences, receive a mostly similar set of PFC inputs. Thus, fewer neurons within individual PFC regions project to midline VTA nuclei and the PN compared to those projecting to the PBP. These findings are well in line with those of former conventional (Geisler and Zahm 2005) and viral tracing studies (Menegas et al. 2015), conceptualizing a brain-wide fairly common set of afferents to VTA, covering all of its subdivisions. In contrast, VTA/SN outputs, particularly those to the entire striatum, are organized topographically, with distinct VTA districts innervating disparate but partly overlapping targets (Breton et al. 2019; Del-Fava et al. 2007; Haber et al. 2000; Ikemoto 2007; Swanson 1982; for review, see also Weele et al. 2019).

Interestingly, such as previously reported for the DR (Gonçalves et al. 2009), we here newly describe FPm as a major source of prefrontal afferents to the VTA, LDTg, and MnR. In rodents, little is known about this cortical area, located at the rostral tip of the cortex. In rats, FPm is strongly interconnected with the remainder PFC (Hoover and Vertes 2007; Murphy and Deutch 2007; Vertes 2004), and has been shown to be densely innervated by the reuniens and rhomboid nuclei of the thalamus (Vertes et al. 2006). Functionally, FPm has been related to the rat motor cortex (Donoghue and Wise 1982; Reep et al. 1987). In humans, the frontal polar cortex (Brodmann area 10) has

been implicated, among other functions (Tsujimoto et al. 2011), in prospective memory (Burgess et al. 2003, Volle et al. 2011). Given that our past (Gonçalves et al. 2009) and present findings highlight FPm as a major input source of state setting neuromodulatory monoaminergic and cholinergic nuclei, this often overlooked tiny part of the rodent PFC clearly deserves further investigation.

When comparing our findings to those of pioneer transmitter-specific viral tracing studies (Ogawa et al. 2014; Watabe-Uchida et al. 2012) that examined whole-brain direct inputs to DA neurons in the VTA-nigra complex, their low numbers of VTA inputs from mPFC subregions such as IL and PrL immediately attracts attention. There is now overwhelming evidence that the VTA, beside DA-only, contains large fractions of GLU-only or GABA-only neurons, as well as neurons with mixed phenotypes (Nair-Roberts et al. 2008; for review, see Morales and Margolis 2017), which all give rise to long-range projections (Breton et al. 2019; Taylor et al. 2014). Thus, as stated by Watabe–Uchida et al. (2012), one scenario to explain this discrepancy is that previous non-viral tracing findings, inclusive ours, may be explained by a large number of mPFC inputs to non-DA neurons in the VTA. Noteworthy, consecutive viral tracing studies, even reporting partly segregated output channels for VTA DA neurons (Beier et al. 2015, 2019), highlighted qualitatively similar inputs to VTA DA (Menegas et al. 2015), GABA, and GLU neurons from several sources, with cortical regions providing a greater share of input to VTA GLU neurons (Faget et al 2016). Another divergence of our findings with those of Watabe-Uchida et al. (2012) is that these authors detected several VTA-projecting neurons in M1 and SI, whereas we rarely observed CTb+ neurons in these cortical fields. This discrepancy may be due to a possible uptake of virus by SNC DA cells in their material. In line with this view, in our material we also observed elevated numbers of CTb+ neurons in M1 and S1, however only in a case in

which the CTb injection had encroached onto SNC. Importantly, the findings from viral tracing studies fully collaborated with one of our key results, the modest number of VTA-projecting neurons in non-PFC cortical fields. Thus, except of rostral parts of S1/M1, only few other cortical regions such as the DP, cingulate-, and retrosplenial cortex were reported to contain some label following virus injections into VTA (Ogawa et al. 2014; Watabe-Uchida et al. 2012).

With regard to prefrontal afferents to LDTg, our current findings point to more substantial and widespread PFC inputs to LDTg than noticed previously (Cornwall et al. 1990, Satoh and Fibiger 1986; Semba and Fibiger 1992). As discussed in detail in a foregoing study (Bueno et al. 2019), we can speculate that these discrepancies are mainly due to the superior sensitivity of CTb in comparison to wheat germ agglutinin-conjugated to horseradish peroxidase (WGA-HRP) or unconjugated WGA, which were used in the above cited pioneer studies. Importantly, our retrograde tracing findings are largely supported by anterograde tracing studies, disclosing that all mPFC subregions (Sesack e al. 1989; Vertes 2004), as well as MO and VO (Hoover and Vertes, 2011) project to LDTg. Moreover, our findings are also in line with a recent study examining whole-brain inputs to different cell types in the LDTg (Wang et al. 2019). These authors described robust cortical inputs to LDTg mostly emerging from VO, PrL, and cingulate cortices, further specifying that cortical regions preferentially target glutamatergic LDTg neurons expressing the vesicular glutamate receptor type 2 (VGLUT2).

Our present findings disclosed that among all injected structures, MnR receives the most robust set of afferents from PFC. In all, this finding is in line with a conventional retrograde tracing study (Behzadi et al. 1990), describing rich cortical label in glutamatergic layer V neurons of the mPFC, midcingulate, and retrosplenial cortex following CTb injections into MnR. Moreover, fully confirming our finding of MO as a

main source of prefrontal afferents to MnR, Hoover and Vertes (2011) illustrated compact anterograde labeling in MnR (see their Figure 12) following injections of the anterograde tracer *Phaseolus vulgaris*-leucoagglutinin (PHA-L) into MO. Similarly, our description of anterior and mid-rostral cingulate areas as a considerable source of input to MnR is fully corroborated by a recent anterograde tract tracing study in mice (Fillinger et al. 2017). Again, our findings of rich mPFC inputs to MnR are only partly in line with those from viral tracing studies examining whole-brain inputs to 5-HT DR/MnR neurons (Ogawa et al. 2014; Pollak Dorocic et al. 2014; see also Sparta and Stuber 2014). Similar to whole-brain input analyses to VTA DA neurons (Ogawa et al. 2014; Watabe-Uchida et al. 2012), it was concluded that mPFC does not provide a particularly heavy input to 5-HT MnR neurons. Nevertheless, in line with our findings, prefrontal fields such as the IL, PrL, and agranular insular areas (Pollak Dorocic et al. 2014) as well as more caudally situated cingulate and retrosplenial areas were identified as principal sources of cortical input to MnR 5-HT neurons (Ogawa et al. 2014; Pollak Dorocic et al. 2014). On the other hand, sharply in contrast with our findings these authors also illustrate somatomotor areas among the principal cortical sources of input to MnR 5-HT neurons. We can only speculate about the factors behind these conflicting results. It is now well established that neurons with a 5-HT-only phenotype form a small minority within MnR, whereas neurons with a glutamatergic (VGLUT3), mixed 5-HT/VGLUT3, GABA-only or unknown phenotype are more common (Hioki et al. 2010; Ren et al. 2019; Sos et al. 2017). Presumably, 5-HT cell-specific viral tracing studies missed mPFC inputs to the abundant non-5-HT neuronal populations within MnR, whereas our findings include them. This fact might explain our robust CTb labeling in mPFC subregions. Regarding the strong additional labeling in somatomotor areas described in viral tracing studies, some caveats have meanwhile been pointed up,

which can potentially account for false negative or positive findings in transsynaptic viral tracing experiments (Rogers and Beier 2021). These include a commonly low input labeling efficiency of about 5% (e.g. DeNardo et al. 2015), biased transneuronal transmission among different types of synapses (Wall et al. 2013), excessive extent of viral injections (see discussion in Nasirova et al. 2021), and Cre expression in unintentionally targeted cells in transgenic mouse lines (Lammel et al. 2015).

Comparison with previous studies on prefrontal inputs to DR and LC

Till yet, among all state-setting neuromodulatory monoamine nuclei, prefrontal inputs to DR have been most thoroughly investigated (e.g. Jankowski and Sesack 2004; Peyron et al. 1998; Weissbourd et al. 2014), inclusive by our group using the same methodology applied here (Gonçalves et al. 2009). Consequently, it is relevant to discuss our findings on PFC afferents to VTA; LDTg, and MnR in relation to earlier findings on DR. Comparing our present results with those of previous conventional tracing studies on prefrontal afferents to DR, several major points attract attention. The bulk of cortical afferents to DR were described to emerge from an essentially similar broad set of PFC regions than reported here for PFC inputs to VTA, LDTg, and MnR. Thus, similar as we detail here, IL, the ventral half of PrL, MO, and FPm were highlighted as major sources of PFC afferents to DR (Gonçalves et al. 2009; Peyron et al. 1998), with Gabbott et al. (2005) additionally depicting robust inputs from Cg1 and M2. Moreover, consistent with the present observations, prior studies on DR also detected only few supplementary cortical inputs to DR, mainly emerging from DP and mid-cingulate areas, and emphasized PFC's distinctive role as the foremost source of cortical afferents to DR and other brainstem state setting neuromodulatory nuclei (Gonçalves et al. 2009; Heidbreder and Groenewegen 2003). Importantly, whereas PFCs afferents to different VTA subdivisions were described to be distributed rather

homogeneous (present findings; Geisler and Zahm, 2005; Menegas et al. 2015), distinct PFC input patterns were reported for rostral, lateral, and caudal DR subdivisions (Commons 2015; Gonçalves et al. 2009; Peyron et al. 1998).

Furthermore, as gleaned from the histograms and charts of former studies (Gonçalves et al. 2009; Peyron et al. 1998), DR and MnR receive a qualitatively highly similar set of inputs from PFC, however with apparently more MnR-projecting neurons found in matching mPFC regions compared to DR-projecting neurons. This observation seems partially at odds with findings from viral tracing studies comparing the organization of monosynaptic inputs to DR and MnR, (Ogawa et al. 2014; Pollak Dorocic et al. 2014). These studies report that most mPFC and oPFC subfields provide stronger inputs to DR 5-HT neurons, whereas, in line with our findings, MnR 5-HT neurons receive more substantial input from mid-cingulate and retrosplenial areas. However, DR 5-HT neurons have been reported to be about 3 times more numerous than their counterparts in the MnR (Vertes and Crane 1997), in which GABA-only, GLU-only, and neurons with a still unknown phenotype prevail (Sos et al. 2017). Thus the elevated numbers of CTb+ PFC neurons in our material may be due to CTb uptake by these latter classes of MnR neurons. Moreover, our finding of a rich innervation of the MnR by the mPFC and mid-cingulate areas is fully in line with the concept that MnR predominantly receives input from (Ogawa and Watabe-Uchida 2018), and projects to (Vertes et al. 1999), structures located near the midline. Noteworthy, the ascending MnR projections to mPFC have been reported to be mainly glutamatergic, with some individual MnR neurons innervating simultaneously the mPFC and hippocampus (Szönyi et al. 2016).

In line with our observation of prominent retrograde labeling in area λ following CTb injections into VTA, LDTg, and MnR, clustered retrograde labeling in this region was already reported in previous studies on prefrontal afferents to DR. (Gonçalves et al.

2009; Peyron et al. 1998). Peyron et al. (1998; see their Figure 8C) described the retrograde labeling within this region dorsally to AcbRP to belong to VO. Concordantly, Swanson in his atlas (1992) also considered this region making part of VO. However, the cell-poor character, and distinct morphology/orientation of its neurons, shed doubt on the view that CTb labeling in area λ can be attributed to any cortical region in the vicinity of the AcbRP. Further in depth connectional, molecular, genetic fate-mapping and functional studies are needed to fully characterize this region. Noteworthy, the DP medially adjacent to area λ was also consistently robustly labeled following CTb injections into VTA, LDTg, and MnR. This finding is in line with those of previous anterograde tracing studies (Akhter et al. 2014; Hurley et al. 1991). Interestingly, a cortical district encompassing the DP/dorsal tenia tecta has been identified to be involved in sustained and selective visual attention (Maddux and Holland 2011) and psychosocial stress responses (Kataoka et al. 2020) in rats.

The noradrenergic LC is another major mesopontine neuromodulatory nucleus previously shown to receive most of its cortical input from PFC (Cedarbaum and Aghajanian 1978; Luppi et al. 1995). Interestingly, PFC top-down projections to the LC have been shown to be more substantial in monkeys than in rodents (Arnsten and Goldman-Rakic 1984; Aston-Jones and Cohen 2005), and in both animal groups primarily terminate in the pericerulear dendritic zone of the LC (Aston-Jones et al. 2004). Functionally, electrophysiological/pharmacological studies in rats revealed, that glutamatergic mPFC neurons provide a potent modulatory influence on the LC, with chemical activation of the mPFC augmenting, and inactivation of the mPFC suppressing the firing of LC neurons (Jodo and Aston-Jones 1997; Jodo et al. 1998).

Functional Considerations

Similar as described in previous studies on prefrontal afferents to DR (Gonçalves et al. 2009; Peyron et al. 1998), we here identified ventral mPFC subregions, namely IL and the ventral part of PrL, together with MO/VO, to contribute most to prefrontal top-down projections to VTA, LDTg, and MnR. The concept of a functional/hodological dorsal-ventral gradient in the rodent mPFC is now broadly acknowledged (Gabbott et al. 2005; Heidbreder and Groenewegen 2003). Thus, ventral mPFC is considered to make part of a medial network mainly concerned with visceromotor functions (Neafsey 1990; Ongur and Price 2000), whereas dorsal mPFC subregions, such as Cg1, M2, and the dorsal part of PrL are believed to be predominantly involved in cognitive and motor functions relevant for the control of actions (Euston et al. 2012; Groenewegen and Uylings 2000). The particularly rich reciprocal interconnections of IL with the hypothalamus (Heidbreder and Groenewegen 2003), and of PL with the central and basolateral amygdala (Vertes 2004), as well as VTA, DR, and MnR (present findings; Vertes 2004), make ventral mPFC a hub with privileged access to information about the acute homeostatic, emotional, and motivational state of an individual, respectively (Euston et al. 2012). Furthermore, the medial oPFC subregions MO and VO, considered serving as a link between oPFC and mPFC (Hoover and Vertes 2011), also substantially contribute to PFC top-down projections to VTA, LDTg, and MnR. The medial oPFC is first of all characterized by its rich access to multimodal sensory information (Ongur and Price, 2000), with specific ensembles of oPFC cells responding to the affective (reward) value of an stimulus in rats (Schoenbaum and Eichenbaum, 1995, van Duuren et al. 2008) and primates (Rolls 2004). Having in mind these considerations, it is conceivable that prefrontal top-down projections from mPFC and oPFC to state-setting mesopontine neuromodulatory nuclei constitute one of the key tracks underlying

possible supervisor (switch operator; Miller and Cohen, 2021) functions of the PFC by constantly adjusting inappropriate behaviors and promoting task and cue relevant ones (Groenewegen and Uylings 2000; Ragozzino et al. 1999; Weele et al 2019).

The here highlighted substantially similar distribution of retrogradely labeled PFC cells, resulting from CTb injections into VTA, LDTg, and MnR, evidently raises the question, whether single PFC neurons might target more than one state setting neuromodulatory cell group. Till yet, there is only limited and somewhat contradictory information about collateralized projections of individual PFC cells. Thus, previous double retrograde tracing studies, investigating several pairs of target regions but not pairs of structures investigated here, reported a relatively low extent of collateralization of mPFC neurons ranging from 2% (VTA/DR; Gabbott et al. 2005) to 14% (Acb/contralateral PFC; Pinto and Sesack 2000). In contrast, Vázquez-Borsetti et al (2010) demonstrated by double-retrograde tracing, as well as antidromic activation from VTA/DR, that up to 60% of mPFC neurons simultaneously project to both monoaminergic cell groups. These and other findings (Bortolozzi et al. 2005; Pehek et al. 2006) indicate that the mPFC might simultaneously impact DA and 5-HT cell groups, supporting a concerted modulation of ascending serotonergic and dopaminergic activity during antipsychotic drug treatment (Vázquez-Borsetti et al. 2010).

Role of prefrontal top-down projections in psychiatric disease

The mechanisms underlying the fine-tuning of PFC function by ascending modulatory catecholaminergic and cholinergic inputs under normal conditions and in psychiatric disease have been intensively investigated (for review, see Arnsten 2011; Arnsten et al. 2012, 2015; Bloem et al. 2014; Cools and Arnsten 2021; Celada et al. 2013; Clark et al. 2004; Galvin et al. 2020; Lapish et al. 2007; Puig and Gulledge 2011; Seamans and Yang 2004; Wallace and Bertrand 2013).

Conversely, although a vital role for prefrontal top-down projections in executive control, mainly via the integration and constant update of bottom-up signals over longer timescales has now been widely acknowledged (Buschman and Miller 2007; Kamigaki 2019, Miller and Cohen 2001), very few studies have hitherto explicitly challenged the role of PFC projections to mesopontine monoaminergic and cholinergic nuclei in executive control. Till yet, specific functions, in mood regulation and coping with stress, have mainly been attributed to PFC projections targeting the DR. Thus, Warden et al (2012) in a technically challenging study, combining single-unit electrophysiology and optogenetics in freely moving rats, observed that selective activation of DR-projecting mPFC neurons rapidly switches the behavior in a forced swim test from passive coping to mobility, suggesting that reduced activity in the mPFC - DR projection might be an important factor favoring passive coping in depression. Fully in line with this, Amat et al (2005, 2008) showed that pharmacologic inactivation of the PL/IL mPFC subregions during stressor exposure eliminates the stressor–resistance produced by control, whereas activation of these mPFC subregions mimics behavioral control and abolishes the increase of 5-HT in the DR that normally occurs during uncontrollable stress. Beside 5-HT, DA is now recognized as another monoamine neurotransmitter involved in the pathophysiology of major depressive disorder (MDD; Chaudhury et al. 2015; Dunlop and Nemeroff 2007; Kaufling 2019; Knowland and Lim 2017; Nestler and Carlezon 2006), with DA-dependent deficits in reward-processing discussed to be particularly relevant in anhedonia (Rizvi et al. 2017; Wang et al. 2021), one of the core syndromes in MDD (Pizzagalli 2014). Interestingly, optogenetic stimulation of mPFC in susceptible mice has antidepressant effects (Covington et al. 2010). However, only little is known about the precise role of mPFC top-down projections to VTA in MDD. In a functional magnetic resonance imaging study in

humans, Young et al. (2016) detected that, anhedonia was related to reduced mPFC connectivity with reward- and emotion-related brain regions. Moreover, Chaudhury et al. (2013) reported that optogenetic activation of mPFC-projecting VTA DA neurons exerted proresilience effects in mice, whereas their inhibition promoted susceptibility. Given that glutamatergic mPFC VTA-projecting neurons have been shown to primarily target VTA DA neurons that project back to mPFC (Carr and Sesack 2000), it is worth testing, whether stimulating the mPFC-VTA pathway might have an antidepressant net effect. Interestingly, dopaminergic functions in the VTA can also be modulated distally by the complex actions of 5-HT on monoamine receptors in the mPFC, particularly via postsynaptic 5-HT_{1A} and 5-HT_{2A} receptors, which are abundantly co-expressed in layer V pyramidal neurons (Santana and Artigas 2017). Activation of 5-HT_{2A} receptors in mPFC enhances dopaminergic activity in the VTA and PFC, indicating that the activity of VTA DA neurons is under the excitatory control of 5-HT_{2A} receptors in the mPFC (Bortolozzi et al. 2005). Altogether, there is now manifold evidence that the 5-HT induced modulation of PFC networks, linking mPFC with VTA and/or DR, are profoundly involved in the actions of antidepressant/antipsychotic (Artigas 2010; Puig et al. 2004), as well as hallucinogenic (Kargieman et al. 2007; Riga et al. 2014) drugs.

Other major controllers of state setting mesopontine modulatory cell groups

Beside the PFC (present findings, Heidbreder and Gronewegen 2003), two subcortical structures, the anterior/lateral hypothalamus and LHb stand out as major controllers of state setting mesopontine modulatory cell groups (Zhou et al. 2017). Thus, mainly preoptic and lateral hypothalamic fields (Geisler and Zahm 2005; Papp and Palkovits 2014), and the medial half of the LHb (Metzger et al. 2017, 2021; Zahm and Root 2017), are robustly interconnected with VTA, DR, MnR, and LDTg. The hypothalamus, via specific glutamatergic and GABAergic neuronal populations

(Bonavion et al. 2016; Geisler et al 2007; Godfrey and Borgland 2019), which often act in an antagonistic manner (Gordon-Fennell and Stuber 2021; Nieh et al. 2015, 2016), multiplexed with neuropeptides such as orexin (Aston-Jones et al. 2009), drives motivated behaviors by means of accurate information about the internal state of the organism (Berthoud and Munzberg 2011; Stuber and Wise 2016). LHb, through parallel topographically organized direct glutamatergic projections (Brinschwitz et al. 2010; Gonçalves et al. 2012; Herkenham and Nauta 1978), and indirectly via the GABAergic rostromedial tegmental nucleus (RMTg; Jhou et al. 2009; Sego et al. 2014), primarily feed-forwards non-reward related information to VTA and DR. Accordingly, key roles in depression (Caldecott-Hazard et al. 1988; Li et al. 2011) and in the mediation of aversive actions of drugs of abuse (Jhou et al. 2013; Kang et al. 2018), together with more general functions in behavioral flexibility/learning (Baker and Mizumori 2017; Mathis and Lecourtier 2017), have now been attributed to LHb (for review, see Hu et al. 2020; Proulx et al. 2014).

Noteworthy, PFC is also in a position to drive mesopontine modulatory cell groups indirectly. Thus, mPFC and oPFC emit relative weak projections to LHb (Kim and Lee 2012) and robust ones to the lateral hypothalamus (Gabbott et al. 2005). Moreover, mPFC can modulate VTA via synaptic relays in the ventrolateral striatum and ventral pallidum (Groenewegen et al. 1993, 1999). More in depth anatomo-functional studies, which might also cover the hitherto understudied LDTg and MnR, are needed to interrogate the specific role of distinct components/pathways within this complex network of top-down controllers of mesopontine modulatory cell groups.

Acknowledgements The authors thank Ana M.P. Campos for expert technical assistance and Mario Costa Cruz for help with confocal microscopy procedures.

Funding Preparation of this manuscript was supported by grants from the Fundação de Amparo à Pesquisa do Estado de São Paulo –FAPESP: Grant numbers 2017/16473-6 (M.M.) and 2020/001318-8 (J.D.J.).

Conflicts of Interest

The authors declare that they have no conflict of interest.

Data Accessibility

The data that support the findings of this study are available from the corresponding author upon reasonable request.

Author Contributions

Study concept and design: M.M., R.S. Acquisition of data: M.M., R.S., D.B., L.G., L.B.L., J.D. Jr., S.J.S-L. Drafting of the manuscript: M.M., R.S., J.D. Jr., S.J.S-L. Critical revision of the manuscript for important intellectual content: M.M., R.S., L.G., L.B.L., D.B., J.D. Jr., S.J.S-L. Obtained funding: M.M., J.D. Jr.

Ethics approval All the procedures were approved by the ethical committee of animal experimentation of the Institute of Biomedical Sciences of the University of São Paulo and were in accordance with the NIH Guidelines for the Use and Care of Laboratory Animals.

Code availability N/A

Consent to participate N/A

Consent for publication N/A

References

Abela AR, Browne CJ, Sargin D, Prevot TD, Ji XD, Li Z, Lambe EK, Fletcher PJ (2020) Median raphe serotonin neurons promote anxiety-like behavior via inputs to the dorsal hippocampus. Neuropharmacology 168:107985. doi:10.1016/j.neuropharm.2020.107985

Ahrlund-Richter S, Xuan Y, van Lunteren JA, Kim H, Ortiz C, Dorocic IP, Meletis K, Carlén M (2019) A whole-brain atlas of monosynaptic input targeting four different cell types in the medial prefrontal cortex of the mouse. Nat Neurosci 22:. 657-668. doi:10.1038/s41593-019-0354-y

Akhter F, Haque T, Sato F, Kato T, Ohara H, Fujio T, Tsutsumi K, Uchino K, Sessle BJ, Yoshida A (2014) Projections from the dorsal peduncular cortex to the trigeminal subnucleus caudalis (medullary dorsal horn) and other lower brainstem areas in rats. Neuroscience 266:23-37. doi:10.1016/j.neuroscience.2014.01.046

Amat J, Baratta MV, Paul E, Bland ST, Watkins LR, Maier SF (2005) Medial prefrontal cortex determines how stressor controllability affects behavior and dorsal raphe nucleus. Nat Neurosci 8:365-371. doi:10.1038/nn1399

Amat J, Paul E, Watkins LR, Maier SF (2008) Activation of the ventral medial prefrontal cortex during an uncontrollable stressor reproduces both the immediate and long-term protective effects of behavioral control. Neuroscience 154:1178-1186. doi:10.1016/j.neuroscience.2008.04.005

Anastasiades PG, Carter AG (2021) Circuit organization of the rodent medial prefrontal cortex. Trends Neurosci 44:550-563. doi:10.1016/j.tins.2021.03.006

Andrade TG, Zangrossi H, Jr., Graeff FG (2013) The median raphe nucleus in anxiety revisited. J Psychopharmacol 27:1107-1115. doi:10.1177/0269881113499208

Arnsten AF (2011) Catecholamine influences on dorsolateral prefrontal cortical networks. Biol Psychiatry 69:e89-99. doi:10.1016/j.biopsych.2011.01.027

Arnsten AF, Goldman-Rakic PS (1984) Selective prefrontal cortical projections to the region of the locus coeruleus and raphe nuclei in the rhesus monkey. Brain Res 306:9-18. doi:10.1016/0006-8993(84)90351-2

Arnsten AF, Wang MJ, Paspalas CD (2012) Neuromodulation of thought: flexibilities and vulnerabilities in prefrontal cortical network synapses. Neuron 76:223-239. doi:10.1016/j.neuron.2012.08.038

Arnsten AF, Wang M, Paspalas CD (2015) Dopamine's actions in primate prefrontal cortex: Challenges for treating cognitive disorders. Pharmacol Rev 67:681-696. doi:10.1124/pr.115.010512

Artigas F (2010) The prefrontal cortex: a target for antipsychotic drugs. Acta Psychiatr Scand 121:11-21. doi:10.1111/j.1600-0447.2009.01455.x

Aston-Jones G, Cohen JD (2005) Adaptive gain and the role of the locus coeruleus-norepinephrine system in optimal performance. J Comp Neurol 493:99-110. doi:10.1002/cne.20723

Aston-Jones G, Smith RJ, Moorman DE, Richardson KA (2009) Role of lateral hypothalamic orexin neurons in reward processing and addiction. Neuropharmacology 56:112-121. doi:10.1016/j.neuropharm.2008.06.060

Aston-Jones G, Zhu Y, Card JP (2004) Numerous GABAergic afferents to locus ceruleus in the pericerulear dendritic zone: possible interneuronal pool. J Neurosci 24:2313-2321. doi:10.1523/JNEUROSCI.5339-03.2004

Baker PM, Mizumori SJY (2017) Control of behavioral flexibility by the lateral habenula. Pharmacol Biochem Behav 162:62-68. doi:10.1016/j.pbb.2017.07.012

Bang SJ, Commons KG (2012) Forebrain GABAergic projections from the dorsal raphe nucleus identified by using GAD67-GFP knock-in mice. J Comp Neurol 520:4157-4167. doi:10.1002/cne.23146

Barker DJ, Root DH, Zhang S, Morales M (2016) Multiplexed neurochemical signaling by neurons of the ventral tegmental area. J Chem Neuroanat 73:33-42. doi:10.1016/j.jchemneu.2015.12.016

Barrot M (2014) The ventral tegmentum and dopamine: A new wave of diversity. Neuroscience 282:243-247. doi:10.1016/j.neuroscience.2014.10.017

Bechara A, Damasio AR (2005) The somatic marker hypothesis: A neural theory of economic decision. Game Econ Behav 52:336-372. doi:10.1016/j.geb.2004.06.010

Behzadi G, Kalen P, Parvopassu F, Wiklund L (1990) Afferents to the median raphe nucleus of the rat - retrograde cholera-toxin and wheat-germ conjugated horseradish-peroxidase tracing, and selective D-[H-3]Aspartate labeling of possible excitatory amino-acid inputs. Neuroscience 37:77-100. doi:10.1016/0306-4522(90)90194-9

Beier KT, Gao XJ, Xie S, DeLoach KE, Malenka RC, Luo L (2019) Topological organization of ventral tegmental area connectivity revealed by viral-genetic dissection of input-output relations. Cell Rep 26:159-167 e156. doi:10.1016/j.celrep.2018.12.040

Beier KT, Steinberg EE, DeLoach KE, Xie S, Miyamichi K, Schwarz L, Gao XJ, Kremer EJ, Malenka RC, Luo L (2015) Circuit architecture of VTA dopamine neurons revealed by systematic input-output mapping. Cell 162:622-634. doi:10.1016/j.cell.2015.07.015

Berthoud HR, Munzberg H (2011) The lateral hypothalamus as integrator of metabolic and environmental needs: from electrical self-stimulation to opto-genetics. Physiol Behav 104:29-39. doi:10.1016/j.physbeh.2011.04.051

Bjorklund A, Dunnett SB (2007) Dopamine neuron systems in the brain: an update. Trends Neurosci 30:194-202. doi:10.1016/j.tins.2007.03.006

Bloem B, Poorthuis RB, Mansvelder HD (2014) Cholinergic modulation of the medial prefrontal cortex: the role of nicotinic receptors in attention and regulation of neuronal activity. Front Neural Circuits 8:17. doi:10.3389/fncir.2014.00017

Bonnavion P, Mickelsen LE, Fujita A, de Lecea L, Jackson AC (2016) Hubs and spokes of the lateral hypothalamus: cell types, circuits and behaviour. J Physiol 594:6443-6462. doi:10.1113/JP271946

Bortolozzi A, Diaz-Mataix L, Scorza MC, Celada P, Artigas F (2005) The activation of 5-HT receptors in prefrontal cortex enhances dopaminergic activity. J Neurochem 95:1597-1607. doi:10.1111/j.1471-4159.2005.03485.x

Bueno D, Lima LB, Souza R, Goncalves L, Leite F, Souza S, Furigo IC, Donato J, Jr., Metzger M (2019) Connections of the laterodorsal tegmental nucleus with the habenular-interpeduncular-raphe system. J Comp Neurol 527:3046-3072. doi:10.1002/cne.24729

Burgess PW, Scott SK, Frith CD (2003) The role of the rostral frontal cortex (area 10) in prospective memory: a lateral versus medial dissociation. Neuropsychologia 41:906-918. doi:10.1016/s0028-3932(02)00327-5

Buschman TJ, Miller EK (2007) Top-down versus bottom-up control of attention in the prefrontal and posterior parietal cortices. Science 315:1860-1862. doi:10.1126/science.1138071

Breton JM, Charbit AR, Snyder BJ, Fong PTK, Dias EV, Himmels P, Lock H, Margolis EB (2019) Relative contributions and mapping of ventral tegmental area dopamine and GABA neurons by projection target in the rat. J Comp Neurol 527:916-941. doi:10.1002/cne.24572

Brinschwitz K, Dittgen A, Madai VI, Lommel R, Geisler S, Veh RW (2010) Glutamatergic axons from the lateral habenula mainly terminate on GABAergic neurons of the ventral midbrain. Neuroscience 168:463-476. doi:10.1016/j.neuroscience.2010.03.050

Caldecotthazard S, Mazziotta J, Phelps M (1988) Cerebral correlates of depressed behavior in rats, visualized using C-14 2-deoxyglucose autoradiography. Journal of Neuroscience 8:1951-1961. doi: 10.1523/JNEUROSCI.08-06-01951.1988

Carlén M (2017) What constitutes the prefrontal cortex? Science 358:478-482. doi:10.1126/science.aan8868

Carr DB, Sesack SR (2000) Projections from the rat prefrontal cortex to the ventral tegmental area: target specificity in the synaptic associations with mesoaccumbens and mesocortical neurons. J Neurosci 20:3864-3873. doi:10.1523/JNEUROSCI.20-10-03864.2000

Cedarbaum JM, Aghajanian GK (1978) Afferent projections to the rat locus coeruleus as determined by a retrograde tracing technique. Journal of Comparative Neurology 178:1-15. doi: 10.1002/cne.901780102

Celada P, Puig MV, Casanovas JM, Guillazo G, Artigas F (2001) Control of dorsal raphe serotonergic neurons by the medial prefrontal cortex: Involvement of serotonin-1A, GABA(A), and glutamate receptors. J Neurosci 21:9917-9929. doi:10.1523/Jneurosci.21-24-09917.2001

Celada P, Puig MV, Artigas F (2013) Serotonin modulation of cortical neurons and networks. Front Integr Neurosci 7:25. doi:10.3389/fnint.2013.00025

Challis C, Beck SG, Berton O (2014) Optogenetic modulation of descending prefrontocortical inputs to the dorsal raphe bidirectionally bias socioaffective choices after social defeat. Front Behav Neurosci 8. doi: 10.3389/fnbeh.2014.00043

Chaudhury D, Liu H, Han MH (2015) Neuronal correlates of depression. Cell Mol Life Sci 72:4825-4848. doi:10.1007/s00018-015-2044-6

Chaudhury D, Walsh JJ, Friedman AK, Juarez B, Ku SM, Koo JW, Ferguson D, Tsai HC, Pomeranz L, Christoffel DJ, Nectow AR, Ekstrand M, Domingos A, Mazei-Robison MS, Mouzon E, Lobo MK, Neve RL, Friedman JM, Russo SJ, Deisseroth K, Nestler EJ, Han MH (2013) Rapid regulation of depression-related behaviours by control of midbrain dopamine neurons. Nature 493:532-+. doi:10.1038/nature11713

Chandler DJ, Jensen P, McCall JG, Pickering AE, Schwarz LA, Totah NK (2019) Redefining noradrenergic neuromodulation of behavior: impacts of a modular locus coeruleus architecture. J Neurosci 39:8239-8249. doi:10.1523/JNEUROSCI.1164-19.2019

Clark L, Cools R, Robbins TW (2004) The neuropsychology of ventral prefrontal cortex: decision-making and reversal learning. Brain Cogn 55:41-53. doi:10.1016/S0278-2626(03)00284-7

Commons KG (2015) Two major network domains in the dorsal raphe nucleus. J Comp Neurol 523:1488-1504. doi:10.1002/cne.23748

Commons KG (2020) Dorsal raphe organization. J Chem Neuroanat 110:101868. doi:10.1016/j.jchemneu.2020.101868

Cools R, Arnsten AFT (2021) Neuromodulation of prefrontal cortex cognitive function in primates: the powerful roles of monoamines and acetylcholine. Neuropsychopharmacol. doi:10.1038/s41386-021-01100-8

Cornwall J, Cooper JD, Phillipson OT (1990) Afferent and efferent connections of the laterodorsal tegmental nucleus in the rat. Brain Res Bull 25 :271-284. doi:10.1016/0361-9230(90)90072-8

Covington HE, Lobo MK, Maze I, Vialou V, Hyman JM, Zaman S, LaPlant Q, Mouzon E, Ghose S, Tamminga CA, Neve RL, Deisseroth K, Nestler EJ (2010) Antidepressant effect of optogenetic stimulation of the medial prefrontal cortex. Journal of Neuroscience 30:16082-16090. doi:10.1523/Jneurosci.1731-10.2010

Dalley JW, Cardinal RN, Robbins TW (2004) Prefrontal executive and cognitive functions in rodents: neural and neurochemical substrates. Neurosci Biobehav Rev 28:771-784. doi:10.1016/j.neubiorev.2004.09.006

Dautan D, Souza AS, Huerta-Ocampo I, Valencia M, Assous M, Witten IB, Deisseroth K, Tepper JM, Bolam JP, Gerdjikov TV, Mena-Segovia J (2016) Segregated cholinergic transmission modulates dopamine neurons integrated in distinct functional circuits. Nat Neurosci 19:1025-1033. doi:10.1038/nn.4335

Del-Fava F, Hasue RH, Ferreira JG, Shammah-Lagnado SJ (2007) Efferent connections of the rostral linear nucleus of the ventral tegmental area in the rat. Neuroscience 145 (3):1059-1076. doi:10.1016/j.neuroscience.2006.12.039

Dembrow N, Johnston D (2014) Subcircuit-specific neuromodulation in the prefrontal cortex. Front Neural Circuits 8:54. doi:10.3389/fncir.2014.00054

DeNardo LA, Berns DS, DeLoach K, Luo L (2015) Connectivity of mouse somatosensory and prefrontal cortex examined with trans-synaptic tracing. Nat Neurosci 18:1687-1697. doi:10.1038/nn.4131

Deutch AY (1993) Prefrontal cortical dopamine systems and the elaboration of functional corticostriatal circuits: implications for schizophrenia and Parkinson's disease. J Neural Transm Gen Sect 91:197-221. doi:10.1007/BF01245232

Donoghue JP, Wise SP (1982) The motor cortex of the rat: cytoarchitecture and microstimulation mapping. J Comp Neurol 212:76-88. doi:10.1002/cne.902120106

Dunlop BW, Nemeroff CB (2007) The role of dopamine in the pathophysiology of depression. Arch Gen Psychiat 64:327-337. doi: 10.1001/archpsyc.64.3.327

Euston DR, Gruber AJ, McNaughton BL (2012) The role of medial prefrontal cortex in memory and decision making. Neuron 76:1057-1070. doi:10.1016/j.neuron.2012.12.002

Faget L, Osakada F, Duan J, Ressler R, Johnson AB, Proudfoot JA, Yoo JH, Callaway EM, Hnasko TS (2016) Afferent inputs to neurotransmitter-defined cell types in the ventral tegmental area. Cell Rep 15:2796-2808. doi:10.1016/j.celrep.2016.05.057

Fillinger C, Yalcin I, Barrot M, Veinante P (2018) Efferents of anterior cingulate areas 24a and 24b and midcingulate areas 24a' and 24b' in the mouse. Brain Struct Funct 223:1747-1778. doi:10.1007/s00429-017-1585-x

Floyd NS, Price JL, Ferry AT, Keay KA, Bandler R (2000) Orbitomedial prefrontal cortical projections to distinct longitudinal columns of the periaqueductal gray in the rat. J Comp Neurol 422:556-578. doi:10.1002/1096-9861(20000710)422:4<556::aid-cne6>3.0.co;2-u

Fuster JM (2001) The prefrontal cortex - An update: time is of the essence. Neuron 30:319-333. doi: 10.1016/S0896-6273(01)00285-9

Gabbott PL, Warner TA, Jays PR, Salway P, Busby SJ (2005) Prefrontal cortex in the rat: projections to subcortical autonomic, motor, and limbic centers. J Comp Neurol 492:145-177. doi:10.1002/cne.20738

Galvin VC, Arnsten AFT, Wang M (2020) Involvement of nicotinic receptors in working memory function. Curr Top Behav Neurosci 45:89-99. doi:10.1007/7854_2020_142

Geddes SD, Assadzada S, Lemelin D, Sokolovski A, Bergeron R, Haj-Dahmane S, Beique JC (2016) Target-specific modulation of the descending prefrontal cortex inputs to the dorsal raphe nucleus by cannabinoids. Proc Natl Acad Sci U S A 113:5429-5434. doi:10.1073/pnas.1522754113

Geisler S, Derst C, Veh RW, Zahm DS (2007) Glutamatergic afferents of the ventral tegmental area in the rat. J Neurosci 27:5730-5743. doi:10.1523/JNEUROSCI.0012-07.2007

Geisler S, Zahm DS (2005) Afferents of the ventral tegmental area in the rat-anatomical substratum for integrative functions. J Comp Neurol 490:270-294. doi:10.1002/cne.20668

Geisler S, Zahm DS (2006) Neurotensin afferents of the ventral tegmental area in the rat: [1] re-examination of their origins and [2] responses to acute psychostimulant and antipsychotic drug administration. Eur J Neurosci 24:116-134. doi:10.1111/j.1460-9568.2006.04928.x

Godfrey N, Borgland SL (2019) Diversity in the lateral hypothalamic input to the ventral tegmental area. Neuropharmacology 154:4-12. doi:10.1016/j.neuropharm.2019.05.014

Gonçalves L, Nogueira MI, Shammah-Lagnado SJ, Metzger M (2009) Prefrontal afferents to the dorsal raphe nucleus in the rat. Brain Res Bull 78:240-247. doi:10.1016/j.brainresbull.2008.11.012

Goncalves L, Sego C, Metzger M (2012) Differential projections from the lateral habenula to the rostromedial tegmental nucleus and ventral tegmental area in the rat. J Comp Neurol 520:1278-1300. doi:10.1002/cne.22787

Gonzalez-Maeso J, Weisstaub NV, Zhou M, Chan P, Ivic L, Ang R, Lira A, Bradley-Moore M, Ge Y, Zhou Q, Sealfon SC, Gingrich JA (2007) Hallucinogens recruit specific cortical 5-HT(2A) receptor-mediated signaling pathways to affect behavior. Neuron 53:439-452. doi:10.1016/j.neuron.2007.01.008

Gordon-Fennell A, Stuber GD (2021) Illuminating subcortical GABAergic and glutamatergic circuits for reward and aversion. Neuropharmacology 198:108725. doi:10.1016/j.neuropharm.2021.108725

Graeff FG, Guimaraes FS, De Andrade TG, Deakin JF (1996) Role of 5-HT in stress, anxiety, and depression. Pharmacol Biochem Behav 54:129-141. doi:10.1016/0091-3057(95)02135-3

Groenewegen HJ, Berendse HW, Haber SN (1993) Organization of the output of the ventral striatopallidal system in the rat: ventral pallidal efferents. Neuroscience 57:113-142. doi:10.1016/0306-4522(93)90115-v

Groenewegen HJ, Uylings HB (2000) The prefrontal cortex and the integration of sensory, limbic and autonomic information. Prog Brain Res 126:3-28. doi:10.1016/S0079-6123(00)26003-2

Groenewegen HJ, Wright CI, Beijer AV, Voorn P (1999) Convergence and segregation of ventral striatal inputs and outputs. Ann N Y Acad Sci 877:49-63. doi:10.1111/j.1749-6632.1999.tb09260.x

Haber SN, Fudge JL, McFarland NR (2000) Striatonigrostriatal pathways in primates form an ascending spiral from the shell to the dorsolateral striatum. J Neurosci 20:2369-2382. doi: 10.1523/JNEUROSCI.20-06-02369.2000

Hajós M, Richards CD, Szekely AD, Sharp T (1998) An electrophysiological and neuroanatomical study of the medial prefrontal cortical projection to the midbrain raphe nuclei in the rat. Neuroscience 87:95-108. doi:10.1016/s0306-4522(98)00157-2

Harris KD, Shepherd GM (2015) The neocortical circuit: themes and variations. Nat Neurosci 18:170-181. doi:10.1038/nn.3917

Heidbreder CA, Groenewegen HJ (2003) The medial prefrontal cortex in the rat: evidence for a dorso-ventral distinction based upon functional and anatomical characteristics. Neurosci Biobehav Rev 27:555-579. doi:10.1016/j.neubiorev.2003.09.003

Herkenham M, Nauta WJ (1979) Efferent connections of the habenular nuclei in the rat. J Comp Neurol 187:19-47. doi:10.1002/cne.901870103

Hioki H, Nakamura H, Ma YF, Konno M, Hayakawa T, Nakamura KC, Fujiyama F, Kaneko T (2010) Vesicular glutamate transporter 3-expressing nonserotonergic projection neurons constitute a subregion in the rat midbrain raphe nuclei. J Comp Neurol 518:668-686. doi:10.1002/cne.22237

Hoover WB, Vertes RP (2007) Anatomical analysis of afferent projections to the medial prefrontal cortex in the rat. Brain Struct Funct 212:149-179. doi:10.1007/s00429-007-0150-4

Hu HL, Cui YH, Yang Y (2020) Circuits and functions of the lateral habenula in health and in disease. Nature Reviews Neuroscience 21:277-295. doi:10.1038/s41583-020-0292-4

Hurley KM, Herbert H, Moga MM, Saper CB (1991) Efferent projections of the infralimbic cortex of the rat. J Comp Neurol 308:249-276. doi:10.1002/cne.903080210

Itoh K, Konishi A, Nomura S, Mizuno N, Nakamura Y, Sugimoto T (1979) Application of coupled oxidation reaction to electron microscopic demonstration of

horseradish peroxidase: cobalt-glucose oxidase method. Brain Res 175:341-346. doi:10.1016/0006-8993(79)91013-8

Ikemoto S (2007) Dopamine reward circuitry: two projection systems from the ventral midbrain to the nucleus accumbens-olfactory tubercle complex. Brain Res Rev 56:27-78. doi:10.1016/j.brainresrev.2007.05.004

Jankowski MP, Sesack SR (2004) Prefrontal cortical projections to the rat dorsal raphe nucleus: ultrastructural features and associations with serotonin and gamma-aminobutyric acid neurons. J Comp Neurol 468:518-529. doi:10.1002/cne.10976

Jhou TC, Geisler S, Marinelli M, Degarmo BA, Zahm DS (2009) The mesopontine rostromedial tegmental nucleus: A structure targeted by the lateral habenula that projects to the ventral tegmental area of Tsai and substantia nigra compacta. J Comp Neurol 513:566-596. doi:10.1002/cne.21891

Jhou TC, Good CH, Rowley CS, Xu SP, Wang H, Burnham NW, Hoffman AF, Lupica CR, Ikemoto S (2013) Cocaine drives aversive conditioning via delayed activation of dopamine-responsive habenular and midbrain pathways. J Neurosci 33:7501-7512. doi:10.1523/JNEUROSCI.3634-12.2013

Jodo E, Aston-Jones G (1997) Activation of locus coeruleus by prefrontal cortex is mediated by excitatory amino acid inputs. Brain research 768:327-332. doi: 10.1523/JNEUROSCI.5339-03.2004

Jodo E, Chiang C, Aston-Jones G (1998) Potent excitatory influence of prefrontal cortex activity on noradrenergic locus coeruleus neurons. Neuroscience 83:63-79. doi:10.1016/s0306-4522(97)00372-2

Kalsbeek A, Voorn P, Buijs RM, Pool CW, Uylings HB (1988) Development of the dopaminergic innervation in the prefrontal cortex of the rat. J Comp Neurol 269:58-72. doi:10.1002/cne.902690105

Kamigaki T (2019) Prefrontal circuit organization for executive control. Neurosci Res 140:23-36. doi:10.1016/j.neures.2018.08.017

Kang S, Li J, Bekker A, Ye JH (2018) Rescue of glutamate transport in the lateral habenula alleviates depression- and anxiety-like behaviors in ethanol-withdrawn rats. Neuropharmacology 129:47-56. doi:10.1016/j.neuropharm.2017.11.013

Kargieman L, Santana N, Mengod G, Celada P, Artigas F (2007) Antipsychotic drugs reverse the disruption in prefrontal cortex function produced by NMDA receptor blockade with phencyclidine. Proc Natl Acad Sci U S A 104:14843-14848. doi:10.1073/pnas.0704848104

Kataoka N, Shima Y, Nakajima K, Nakamura K (2020) A central master driver of psychosocial stress responses in the rat. Science 367:1105-1112. doi:10.1126/science.aaz4639

Kaufling J (2019) Alterations and adaptation of ventral tegmental area dopaminergic neurons in animal models of depression. Cell Tissue Res 377:59-71. doi:10.1007/s00441-019-03007-9

Kesner RP, Churchwell JC (2011) An analysis of rat prefrontal cortex in mediating executive function. Neurobiol Learn Mem 96:417-431. doi:10.1016/j.nlm.2011.07.002

Kim U, Lee T (2012) Topography of descending projections from anterior insular and medial prefrontal regions to the lateral habenula of the epithalamus in the rat. Eur J Neurosci 35:1253-1269. doi:10.1111/j.1460-9568.2012.08030.x

Kolb B, Mychasiuk R, Muhammad A, Li Y, Frost DO, Gibb R (2012) Experience and the developing prefrontal cortex. Proc Natl Acad Sci U S A 109 Suppl 2:17186-17193. doi:10.1073/pnas.1121251109

Knowland D, Lim BK (2018) Circuit-based frameworks of depressive behaviors: The role of reward circuitry and beyond. Pharmacol Biochem Behav 174:42-52. doi:10.1016/j.pbb.2017.12.010

Krettek JE, Price JL (1977) The cortical projections of the mediodorsal nucleus and adjacent thalamic nuclei in the rat. J Comp Neurol 171:157-191. doi:10.1002/cne.901710204

Lammel S, Hetzel A, Hackel O, Jones I, Liss B, Roeper J (2008) Unique properties of mesoprefrontal neurons within a dual mesocorticolimbic dopamine system. Neuron 57:760-773. doi:10.1016/j.neuron.2008.01.022

Lammel S, Ion DI, Roeper J, Malenka RC (2011) Projection-specific modulation of dopamine neuron synapses by aversive and rewarding stimuli. Neuron 70:855-862. doi:10.1016/j.neuron.2011.03.025

Lammel S, Lim BK, Malenka RC (2014) Reward and aversion in a heterogeneous midbrain dopamine system. Neuropharmacology 76:351-359. doi:10.1016/j.neuropharm.2013.03.019

Lammel S, Lim BK, Ran C, Huang KW, Betley MJ, Tye KM, Deisseroth K, Malenka RC (2012) Input-specific control of reward and aversion in the ventral tegmental area. Nature 491:212-217. doi:10.1038/nature11527

Lammel S, Steinberg EE, Foldy C, Wall NR, Beier K, Luo L, Malenka RC (2015) Diversity of transgenic mouse models for selective targeting of midbrain dopamine neurons. Neuron 85:429-438. doi:10.1016/j.neuron.2014.12.036

Li B, Piriz J, Mirrione M, Chung C, Proulx CD, Schulz D, Henn F, Malinow R (2011) Synaptic potentiation onto habenula neurons in the learned helplessness model of depression. Nature 470:535-539. doi:10.1038/nature09742

Lima LB, Bueno D, Leite F, Souza S, Goncalves L, Furigo IC, Donato J, Jr., Metzger M (2017) Afferent and efferent connections of the interpeduncular nucleus with special reference to circuits involving the habenula and raphe nuclei. J Comp Neurol 525:2411-2442. doi:10.1002/cne.24217

Lindvall O, Bjorklund A, Nobin A, Stenevi U (1974) The adrenergic innervation of the rat thalamus as revealed by the glyoxylic acid fluorescence method. J Comp Neurol 154:317-347. doi:10.1002/cne.901540307

Lodge DJ (2011) The medial prefrontal and orbitofrontal cortices differentially regulate dopamine system function. Neuropsychopharmacol 36:1227-1236. doi:10.1038/npp.2011.7

Lodge DJ, Grace AA (2006) The laterodorsal tegmentum is essential for burst firing of ventral tegmental area dopamine neurons. Proc Natl Acad Sci U S A 103:5167-5172. doi:10.1073/pnas.0510715103

Loughlin SE, Foote SL, Fallon JH (1982) Locus coeruleus projections to cortex: topography, morphology and collateralization. Brain Res Bull 9:287-294. doi:10.1016/0361-9230(82)90142-3

Luppi PH, Aston-Jones G, Akaoka H, Chouvet G, Jouvet M (1995) Afferent projections to the rat locus coeruleus demonstrated by retrograde and anterograde tracing with cholera-toxin B subunit and Phaseolus vulgaris leucoagglutinin. Neuroscience 65:119-160. doi:10.1016/0306-4522(94)00481-j

Luppi PH, Fort P, Jouvet M (1990) Iontophoretic application of unconjugated cholera toxin B subunit (CTb) combined with immunohistochemistry of neurochemical substances: a method for transmitter identification of retrogradely labeled neurons. Brain Res 534:209-224. doi:10.1016/0006-8993(90)90131-t

Maddux JM, Holland PC (2011) Effects of dorsal or ventral medial prefrontal cortical lesions on five-choice serial reaction time performance in rats. Behav Brain Res 221:63-74. doi:10.1016/j.bbr.2011.02.031

Mathis V, Lecourtier L (2017) Role of the lateral habenula in memory through online processing of information. Pharmacol Biochem Behav 162:69-78. doi:10.1016/j.pbb.2017.07.004

Martin-Ruiz R, Puig MV, Celada P, Shapiro DA, Roth BL, Mengod G, Artigas F (2001) Control of serotonergic function in medial prefrontal cortex by serotonin-2A receptors through a glutamate-dependent mechanism. Journal of Neuroscience 21 :9856-9866. doi:10.1523/Jneurosci.21-24-09856.2001

Menegas W, Bergan JF, Ogawa SK, Isogai Y, Umadevi Venkataraju K, Osten P, Uchida N, Watabe-Uchida M (2015) Dopamine neurons projecting to the posterior striatum form an anatomically distinct subclass. Elife 4:e10032. doi:10.7554/eLife.10032

Mesulam MM, Mufson EJ, Wainer BH, Levey AI (1983) Central cholinergic pathways in the rat: an overview based on an alternative nomenclature (Ch1-Ch6). Neuroscience 10:1185-1201. doi:10.1016/0306-4522(83)90108-2

Metzger M, Bueno D, Lima LB (2017) The lateral habenula and the serotonergic system. Pharmacol Biochem Behav 162:22-28. doi:10.1016/j.pbb.2017.05.007

Metzger M, Souza R, Lima LB, Bueno D, Goncalves L, Sego C, Donato J, Jr., Shammah-Lagnado SJ (2021) Habenular connections with the dopaminergic and serotonergic system and their role in stress-related psychiatric disorders. Eur J Neurosci 53:65-88. doi:10.1111/ejn.14647

Miller EK, Cohen JD (2001) An integrative theory of prefrontal cortex function. Annu Rev Neurosci 24:167-202. doi:10.1146/annurev.neuro.24.1.167

Morales M, Margolis EB (2017) Ventral tegmental area: cellular heterogeneity, connectivity and behaviour. Nat Rev Neurosci 18:73-85. doi:10.1038/nrn.2016.165

Murphy MJM, Deutch AY (2018) Organization of afferents to the orbitofrontal cortex in the rat. J Comp Neurol 526:1498-1526. doi:10.1002/cne.24424

Muzerelle A, Scotto-Lomassese S, Bernard JF, Soiza-Reilly M, Gaspar P (2016) Conditional anterograde tracing reveals distinct targeting of individual serotonin cell groups (B5-B9) to the forebrain and brainstem. Brain Struct Funct 221:535-561. doi:10.1007/s00429-014-0924-4

Nair-Roberts RG, Chatelain-Badie SD, Benson E, White-Cooper H, Bolam JP, Ungless MA (2008) Stereological estimates of dopaminergic, GABAergic and glutamatergic neurons in the ventral tegmental area, substantia nigra and retrorubral field in the rat. Neuroscience 152:1024-1031. doi:10.1016/j.neuroscience.2008.01.046

Nasirova N, Quina LA, Novik S, Turner EE (2021) Genetically targeted connectivity tracing excludes dopaminergic inputs to the interpeduncular nucleus from the ventral tegmentum and substantia nigra. eNeuro 8 (3). doi:10.1523/ENEURO.0127-21.2021

Neafsey EJ (1990) Prefrontal cortical control of the autonomic nervous-system - anatomical and physiological observations. Progress in Brain Research 85:147-166. doi: 10.1016/s0079-6123(08)62679-5

Nestler EJ, Carlezon WA, Jr. (2006) The mesolimbic dopamine reward circuit in depression. Biol Psychiatry 59:1151-1159. doi:10.1016/j.biopsych.2005.09.018

Nieh EH, Matthews GA, Allsop SA, Presbrey KN, Leppla CA, Wichmann R, Neve R, Wildes CP, Tye KM (2015) Decoding neural circuits that control compulsive sucrose seeking. Cell 160:528-541. doi:10.1016/j.cell.2015.01.003

Nieh EH, Vander Weele CM, Matthews GA, Presbrey KN, Wichmann R, Leppla CA, Izadmehr EM, Tye KM (2016) Inhibitory input from the lateral hypothalamus to the ventral tegmental area disinhibits dopamine neurons and promotes behavioral activation. Neuron 90:1286-1298. doi:10.1016/j.neuron.2016.04.035

Ogawa SK, Cohen JY, Hwang D, Uchida N, Watabe-Uchida M (2014) Organization of monosynaptic inputs to the serotonin and dopamine neuromodulatory systems. Cell Rep 8:1105-1118. doi:10.1016/j.celrep.2014.06.042

Ogawa SK, Watabe-Uchida M (2018) Organization of dopamine and serotonin system: Anatomical and functional mapping of monosynaptic inputs using rabies virus. Pharmacol Biochem Behav 174:9-22. doi:10.1016/j.pbb.2017.05.001

Ohmura Y, Tanaka KF, Tsunematsu T, Yamanaka A, Yoshioka M (2014) Optogenetic activation of serotonergic neurons enhances anxiety-like behaviour in mice. Int J Neuropsychopharmacol 17:1777-1783. doi:10.1017/S1461145714000637

Ohmura Y, Tsutsui-Kimura I, Sasamori H, Nebuka M, Nishitani N, Tanaka KF, Yamanaka A, Yoshioka M (2020) Different roles of distinct serotonergic pathways in anxiety-like behavior, antidepressant-like, and anti-impulsive effects. Neuropharmacology 167:107703. doi:10.1016/j.neuropharm.2019.107703

Okaty BW, Sturrock N, Escobedo Lozoya Y, Chang Y, Senft RA, Lyon KA, Alekseyenko OV, Dymecki SM (2020) A single-cell transcriptomic and anatomic atlas of mouse dorsal raphe Pet1 neurons. Elife 9. doi:10.7554/eLife.55523

Ongur D, Price JL (2000) The organization of networks within the orbital and medial prefrontal cortex of rats, monkeys and humans. Cerebral Cortex 10:206-219. doi:DOI 10.1093/cercor/10.3.206

Overton PG, Clark D (1997) Burst firing in midbrain dopaminergic neurons. Brain Res Brain Res Rev 25:312-334. doi:10.1016/s0165-0173(97)00039-8

Overton PG, Tong ZY, Clark D (1996) A pharmacological analysis of the burst events induced in midbrain dopaminergic neurons by electrical stimulation of the prefrontal cortex in the rat. J Neural Transm (Vienna) 103:523-540. doi:10.1007/BF01273151

Paxinos G, Watson C (2007) The rat brain in stereotaxic coordinates: Sixth Edition. Elsevier, Amsterdam

Papp RS, Palkovits M (2014) Brainstem projections of neurons located in various subdivisions of the dorsolateral hypothalamic area-an anterograde tract-tracing study. Front Neuroanat 8. doi:10.3389/fnana.2014.00034

Pehek EA, Nocjar C, Roth BL, Byrd TA, Mabrouk OS (2006) Evidence for the preferential involvement of 5-HT2A serotonin receptors in stress- and drug-induced dopamine release in the rat medial prefrontal cortex. Neuropsychopharmacol 31:265-277. doi:10.1038/sj.npp.1300819

Peyron C, Petit JM, Rampon C, Jouvet M, Luppi PH (1998) Forebrain afferents to the rat dorsal raphe nucleus demonstrated by retrograde and anterograde tracing methods. Neuroscience 82:443-468. doi:10.1016/s0306-4522(97)00268-6

Phillips AG, Vacca G, Ahn S (2008) A top-down perspective on dopamine, motivation and memory. Pharmacol Biochem Behav 90:236-249. doi:10.1016/j.pbb.2007.10.014

Phillipson OT (1979) Afferent projections to the ventral tegmental area of Tsai and interfascicular nucleus: a horseradish peroxidase study in the rat. J Comp Neurol 187:117-143. doi:10.1002/cne.901870108

Pizzagalli DA (2014) Depression, stress, and anhedonia: toward a synthesis and integrated model. Annu Rev Clin Psychol 10:393-423. doi:10.1146/annurev-clinpsy-050212-185606

Pollak Dorocic I, Furth D, Xuan Y, Johansson Y, Pozzi L, Silberberg G, Carlén M, Meletis K (2014) A whole-brain atlas of inputs to serotonergic neurons of the dorsal and median raphe nuclei. Neuron 83:663-678. doi:10.1016/j.neuron.2014.07.002

Proulx CD, Hikosaka O, Malinow R (2014) Reward processing by the lateral habenula in normal and depressive behaviors. Nat Neurosci 1:1146-1152. doi:10.1038/nn.3779

Puig MV, Gulledge AT (2011) Serotonin and prefrontal cortex function: neurons, networks, and circuits. Mol Neurobiol 44:449-464. doi:10.1007/s12035-011-8214-0

Puig MV, Celada P, Artigas F (2004) Serotonergic control of prefrontal cortex. Rev Neurologia 39:539-547. doi:10.33588/rn.3906.2004433

Ragozzino ME (2007) The contribution of the medial prefrontal cortex, orbitofrontal cortex, and dorsomedial striatum to behavioral flexibility. Ann N Y Acad Sci 1121:355-375. doi:10.1196/annals.1401.013

Ragozzino ME, Detrick S, Kesner RP (1999) Involvement of the prelimbic-infralimbic areas of the rodent prefrontal cortex in behavioral flexibility for place and response learning. J Neurosci 19:4585-4594. doi: 10.1523/JNEUROSCI.19-11-04585.1999

Ray JP, Price JL (1992) The organization of the thalamocortical connections of the mediodorsal thalamic nucleus in the rat, related to the ventral forebrain-prefrontal cortex topography. J Comp Neurol 323:167-197. doi:10.1002/cne.903230204

Reep RL, Corwin JV, Hashimoto A, Watson RT (1987) Efferent connections of the rostral portion of medial agranular cortex in rats. Brain Res Bull 19:203-221. doi:10.1016/0361-9230(87)90086-4

Ren J, Isakova A, Friedmann D, Zeng J, Grutzner SM, Pun A, Zhao GQ, Kolluru SS, Wang R, Lin R, Li P, Li A, Raymond JL, Luo Q, Luo M, Quake SR, Luo L (2019) Single-cell transcriptomes and whole-brain projections of serotonin neurons in the mouse dorsal and median raphe nuclei. Elife 8. doi:10.7554/eLife.49424

Rich EL, Shapiro M (2009) Rat prefrontal cortical neurons selectively code strategy switches. J Neurosci 29:7208-7219. doi:10.1523/JNEUROSCI.6068-08.2009

Rich EL, Shapiro ML (2007) Prelimbic/infralimbic inactivation impairs memory for multiple task switches, but not flexible selection of familiar tasks. J Neurosci 27:4747-4755. doi:10.1523/JNEUROSCI.0369-07.2007

Riga MS, Soria G, Tudela R, Artigas F, Celada P (2014) The natural hallucinogen 5-MeO-DMT, component of Ayahuasca, disrupts cortical function in rats: reversal by antipsychotic drugs. Int J Neuropsychopharmacol 17:1269-1282. doi:10.1017/S1461145714000261

Rizvi SJ, Pizzagalli DA, Sproule BA, Kennedy SH (2016) Assessing anhedonia in depression: Potentials and pitfalls. Neurosci Biobehav R 65:21-35. doi:10.1016/j.neubiorev.2016.03.004

Robbins TW (2005) Chemistry of the mind: neurochemical modulation of prefrontal cortical function. J Comp Neurol 493:140-146. doi:10.1002/cne.20717

Rogers A, Beier KT (2021) Can transsynaptic viral strategies be used to reveal functional aspects of neural circuitry? Journal of Neuroscience Methods:109005. doi:10.1016/j.jneumeth.2020.109005

Rolls ET (2004) The functions of the orbitofrontal cortex. Brain Cogn 55:11-29. doi:10.1016/S0278-2626(03)00277-X

Sanchez-Catalan MJ, Kaufling J, Georges F, Veinante P, Barrot M (2014) The antero-posterior heterogeneity of the ventral tegmental area. Neuroscience 282:198-216. doi:10.1016/j.neuroscience.2014.09.025

Santana N, Artigas F (2017) Laminar and cellular distribution of monoamine receptors in rat medial prefrontal cortex. Front Neuroanat 11:87. doi:10.3389/fnana.2017.00087

Saper CB (1984) Organization of cerebral cortical afferent systems in the rat. II. magnocellular basal nucleus. J Comp Neurol 222:313-342. doi:10.1002/cne.902220302

Sargin D, Jeoung HS, Goodfellow NM, Lambe EK (2019) Serotonin regulation of the prefrontal cortex: cognitive relevance and the impact of developmental perturbation. ACS Chem Neurosci 10:3078-3093. doi:10.1021/acschemneuro.9b00073

Satoh K, Fibiger HC (1986) Cholinergic neurons of the laterodorsal tegmental nucleus: efferent and afferent connections. J Comp Neurol 253:277-302. doi:10.1002/cne.902530302

Sawaguchi T, Goldmanrakic PS (1994) The role of D1-dopamine receptor in working-memory - local injections of dopamine antagonists into the prefrontal cortex of rhesus-monkeys performing an oculomotor delayed-response task. J Neurophysiol 71:515-528. doi:10.1152/jn.1994.71.2.515

Schoenbaum G, Eichenbaum H (1995) Information coding in the rodent prefrontal cortex. II. Ensemble activity in orbitofrontal cortex. J Neurophysiol 74:751-762. doi:10.1152/jn.1995.74.2.751

Schwarz LA, Luo L (2015) Organization of the locus coeruleus-norepinephrine system. Curr Biol 25:R1051-R1056. doi:10.1016/j.cub.2015.09.039

Seamans JK, Yang CR (2004) The principal features and mechanisms of dopamine modulation in the prefrontal cortex. Prog Neurobiol 74:1-58. doi:10.1016/j.pneurobio.2004.05.006

Sego C, Goncalves L, Lima L, Furigo IC, Donato J, Jr., Metzger M (2014) Lateral habenula and the rostromedial tegmental nucleus innervate neurochemically distinct subdivisions of the dorsal raphe nucleus in the rat. J Comp Neurol 522:1454-1484. doi:10.1002/cne.23533

Sesack SR, Deutch AY, Roth RH, Bunney BS (1989) Topographical organization of the efferent projections of the medial prefrontal cortex in the rat: an anterograde tract-tracing study with Phaseolus vulgaris leucoagglutinin. J Comp Neurol 290:213-242. doi:10.1002/cne.902900205

Sesack SR, Pickel VM (1992) Prefrontal cortical efferents in the rat synapse on unlabeled neuronal targets of catecholamine terminals in the nucleus accumbens septi and on dopamine neurons in the ventral tegmental area. J Comp Neurol 320:145-160. doi:10.1002/cne.903200202

Soiza-Reilly M, Meye FJ, Olusakin J, Telley L, Petit E, Chen X, Mameli M, Jabaudon D, Sze JY, Gaspar P (2019) SSRIs target prefrontal to raphe circuits during development modulating synaptic connectivity and emotional behavior. Mol Psychiatry 24:726-745. doi:10.1038/s41380-018-0260-9

Sos KE, Mayer MI, Cserep C, Takacs FS, Szonyi A, Freund TF, Nyiri G (2017) Cellular architecture and transmitter phenotypes of neurons of the mouse median raphe region. Brain Struct Funct 222:287-299. doi:10.1007/s00429-016-1217-x

Sparta DR, Stuber GD (2014) Cartography of serotonergic circuits. Neuron 83:513-515. doi:10.1016/j.neuron.2014.07.030

Spruston N (2008) Pyramidal neurons: dendritic structure and synaptic integration. Nat Rev Neurosci 9:206-221. doi:10.1038/nrn2286

Steriade M, Datta S, Pare D, Oakson G, Curro Dossi RC (1990) Neuronal activities in brain-stem cholinergic nuclei related to tonic activation processes in thalamocortical systems. J Neurosci 10:2541-2559. doi:10.1523/JNEUROSCI.10-08-02541.1990

Sternberger LA, Sternberger NH (1983) Monoclonal antibodies distinguish phosphorylated and nonphosphorylated forms of neurofilaments in situ. Proc Natl Acad Sci U S A 80:6126-6130. doi:10.1073/pnas.80.19.6126

Stuber GD, Wise RA (2016) Lateral hypothalamic circuits for feeding and reward. Nat Neurosci 19:198-205. doi:10.1038/nn.4220

Swanson LW (1992) Brain Maps: Structure of the Rat Brain, 1th ed., Elsevier, Los Angeles

Szonyi A, Mayer MI, Cserep C, Takacs VT, Watanabe M, Freund TF, Nyiri G (2016) The ascending median raphe projections are mainly glutamatergic in the mouse forebrain. Brain Struct Funct 221:735-751. doi:10.1007/s00429-014-0935-1

Szonyi A, Zicho K, Barth AM, Gonczi RT, Schlingloff D, Torok B, Sipos E, Major A, Bardoczi Z, Sos KE, Gulyas AI, Varga V, Zelena D, Freund TF, Nyiri G (2019) Median raphe controls acquisition of negative experience in the mouse. Science 366 (6469). doi:10.1126/science.aay8746

Tasic B, Yao Z, Graybuck LT, Smith KA, Nguyen TN, Bertagnolli D, Goldy J, Garren E, Economo MN, Viswanathan S, Penn O, Bakken T, Menon V, Miller J, Fong O, Hirokawa KE, Lathia K, Rimorin C, Tieu M, Larsen R, Casper T, Barkan E, Kroll M, Parry S, Shapovalova NV, Hirschstein D, Pendergraft J, Sullivan HA, Kim TK, Szafer A, Dee N, Groblewski P, Wickersham I, Cetin A, Harris JA, Levi BP, Sunkin SM, Madisen L, Daigle TL, Looger L, Bernard A, Phillips J, Lein E, Hawrylycz M, Svoboda K, Jones AR, Koch C, Zeng H (2018) Shared and distinct transcriptomic cell types across neocortical areas. Nature 563:72-78. doi:10.1038/s41586-018-0654-5

Taylor SR, Badurek S, Dileone RJ, Nashmi R, Minichiello L, Picciotto MR (2014) GABAergic and glutamatergic efferents of the mouse ventral tegmental area. J Comp Neurol 522:3308-3334. doi:10.1002/cne.23603

Teissier A, Chemiakine A, Inbar B, Bagchi S, Ray RS, Palmiter RD, Dymecki SM, Moore H, Ansorge MS (2015) Activity of raphe serotonergic neurons controls emotional behaviors. Cell Rep 13:1965-1976. doi:10.1016/j.celrep.2015.10.061

Tong ZY, Overton PG, Martinez-Cue C, Clark D (1998) Do non-dopaminergic neurons in the ventral tegmental area play a role in the responses elicited in A10 dopaminergic neurons by electrical stimulation of the prefrontal cortex? Exp Brain Res 118:466-476. doi:10.1007/s002210050303

Tsujimoto S, Genovesio A, Wise SP (2011) Frontal pole cortex: encoding ends at the end of the endbrain. Trends Cogn Sci 15:169-176. doi:10.1016/j.tics.2011.02.001

Tulving E, Schacter DL (1995) Memory systems 1994. Mit Press, Cambridge

Van De Werd HJ, Rajkowska G, Evers P, Uylings HB (2010) Cytoarchitectonic and chemoarchitectonic characterization of the prefrontal cortical areas in the mouse. Brain Struct Funct 214:339-353. doi:10.1007/s00429-010-0247-z

Van De Werd HJ, Uylings HB (2008) The rat orbital and agranular insular prefrontal cortical areas: a cytoarchitectonic and chemoarchitectonic study. Brain Struct Funct 212:387-401. doi:10.1007/s00429-007-0164-y

Van Duuren E, Lankelma J, Pennartz CM (2008) Population coding of reward magnitude in the orbitofrontal cortex of the rat. J Neurosci 28:8590-8603. doi:10.1523/JNEUROSCI.5549-07.2008

Van Eden CG, Uylings HB (1985) Cytoarchitectonic development of the prefrontal cortex in the rat. J Comp Neurol 241:253-267. doi:10.1002/cne.902410302

Vazquez-Borsetti P, Cortes R, Artigas F (2009) Pyramidal neurons in rat prefrontal cortex projecting to ventral tegmental area and dorsal raphe nucleus express 5-HT2A receptors. Cereb Cortex 19:1678-1686. doi:10.1093/cercor/bhn204

Vazquez-Borsetti P, Celada P, Cortes R, Artigas F (2011) Simultaneous projections from prefrontal cortex to dopaminergic and serotonergic nuclei. Int J Neuropsychopharmacol 14:289-302. doi:10.1017/S1461145710000349

Verharen JPH, Zhu Y, Lammel S (2020) Aversion hot spots in the dopamine system. Curr Opin Neurobiol 64:46-52. doi:10.1016/j.conb.2020.02.002

Vertes RP (1991) A PHA-L analysis of ascending projections of the dorsal raphe nucleus in the rat. J Comp Neurol 313:643-668. doi:10.1002/cne.903130409

Vertes RP (2004) Differential projections of the infralimbic and prelimbic cortex in the rat. Synapse 51:32-58. doi:10.1002/syn.10279

Vertes RP, Hoover WB, Do Valle AC, Sherman A, Rodriguez JJ (2006) Efferent projections of reuniens and rhomboid nuclei of the thalamus in the rat. J Comp Neurol 499:768-796. doi:10.1002/cne.21135

Vertes RP, Crane AM (1997) Distribution, quantification, and morphological characteristics of serotonin-immunoreactive cells of the supralemniscal nucleus (B9) and pontomesencephalic reticular formation in the rat. J Comp Neurol 378:411-424. doi:10.1002/(sici)1096-9861(19970217)378:3<411::aid-cne8>3.0.co;2-6

Vertes RP, Fortin WJ, Crane AM (1999) Projections of the median raphe nucleus in the rat. J Comp Neurol 407:555-582. PMID: 10235645

Vogt BA, Paxinos G (2014) Cytoarchitecture of mouse and rat cingulate cortex with human homologies. Brain Struct Funct 219:185-192. doi:10.1007/s00429-012-0493-3

Volle E, Gonen-Yaacovi G, Costello Ade L, Gilbert SJ, Burgess PW (2011) The role of rostral prefrontal cortex in prospective memory: a voxel-based lesion study. Neuropsychologia 49:2185-2198. doi:10.1016/j.neuropsychologia.2011.02.045

Wall NR, De La Parra M, Callaway EM, Kreitzer AC (2013) Differential innervation of direct- and indirect-pathway striatal projection neurons. Neuron 79:347-360. doi:10.1016/j.neuron.2013.05.014

Wallace TL, Bertrand D (2013) Importance of the nicotinic acetylcholine receptor system in the prefrontal cortex. Biochem Pharmacol 85:1713-1720. doi:10.1016/j.bcp.2013.04.001

Wang SJ, Leri F, Rizvi SJ (2021) Anhedonia as a central factor in depression: Neural mechanisms revealed from preclinical to clinical evidence. Prog Neuro-Psychoph 110. doi: 10.1016/j.pnpbp.2021.110289

Wang X, Yang H, Pan L, Hao S, Wu X, Zhan L, Liu Y, Meng F, Lou H, Shen Y, Duan S, Wang H (2019) Brain-wide mapping of mono-synaptic afferents to different cell types in the laterodorsal tegmentum. Neurosci Bull 35:781-790. doi:10.1007/s12264-019-00397-2

Warden MR, Selimbeyoglu A, Mirzabekov JJ, Lo M, Thompson KR, Kim SY, Adhikari A, Tye KM, Frank LM, Deisseroth K (2012) A prefrontal cortex-brainstem neuronal projection that controls response to behavioural challenge. Nature 492:428-432. doi:10.1038/nature11617

Watabe-Uchida M, Zhu L, Ogawa SK, Vamanrao A, Uchida N (2012) Whole-brain mapping of direct inputs to midbrain dopamine neurons. Neuron 74:858-873. doi:10.1016/j.neuron.2012.03.017

Weele CMV, Siciliano CA, Tye KM (2019) Dopamine tunes prefrontal outputs to orchestrate aversive processing. Brain Res 1713:16-31. doi:10.1016/j.brainres.2018.11.044

Weissbourd B, Ren J, DeLoach KE, Guenthner CJ, Miyamichi K, Luo L (2014) Presynaptic partners of dorsal raphe serotonergic and GABAergic neurons. Neuron 83:645-662. doi:10.1016/j.neuron.2014.06.024

Wickersham IR, Lyon DC, Barnard RJ, Mori T, Finke S, Conzelmann KK, Young JA, Callaway EM (2007) Monosynaptic restriction of transsynaptic tracing from single, genetically targeted neurons. Neuron 53:639-647. doi:10.1016/j.neuron.2007.01.033

Woolf NJ, Butcher LL (2011) Cholinergic systems mediate action from movement to higher consciousness. Behav Brain Res 221:488-498. doi:10.1016/j.bbr.2009.12.046

Yetnikoff L, Cheng AY, Lavezzi HN, Parsley KP, Zahm DS (2015) Sources of input to the rostromedial tegmental nucleus, ventral tegmental area, and lateral habenula compared: a study in rat. J Comp Neurol 523:2426-2456. doi:10.1002/cne.23797

Young CB, Chen T, Nusslock R, Keller J, Schatzberg AF, Menon V (2016) Anhedonia and general distress show dissociable ventromedial prefrontal cortex connectivity in major depressive disorder. Transl Psychiat 6. doi: 10.1038/tp.2016.80

Zahm DS, Heimer L (1993) Specificity in the efferent projections of the nucleus accumbens in the rat: comparison of the rostral pole projection patterns with those of the core and shell. J Comp Neurol 327:220-232. doi:10.1002/cne.903270205

Zahm DS, Root DH (2017) Review of the cytology and connections of the lateral habenula, an avatar of adaptive behaving. Pharmacol Biochem Behav 162:3-21. doi:10.1016/j.pbb.2017.06.004

Zhou L, Liu MZ, Li Q, Deng J, Mu D, Sun YG (2017) Organization of functional long-range circuits controlling the activity of serotonergic neurons in the dorsal raphe nucleus. Cell Rep 18:3018-3032. doi:10.1016/j.celrep.2017.02.077

Abbreviations:

aca	Anterior commissure, anterior part
Acb	Accumbens nucleus
AcbRP	Accumbens nucleus, rostral pole
AcbSh	Accumbens nucleus, shell
AID	Agranular insular cortex, dorsal part
AIV	Agranular insular cortex, ventral part
cc	Corpus callosum
cg	Cingulum
Cg1	Cingulate cortex, area 1
Cg2	Cingulate cortex, area 2
Cl	Claustrum
CLi	Caudal linear nucleus of the raphe
CPu	Caudate putamen
CTb	Cholera toxin subunit b
DEn	Dorsal endopiriform nucleus
DI	Dysgranular insular cortex
DP	Dorsal peduncular cortex
DR	Dorsal raphe nucleus
DRC	Dorsal raphe nucleus, caudal part
DRD	Dorsal raphe nucleus, dorsal part
DRI	Dorsal raphe nucleus, interstitial part
DRL	Dorsal raphe nucleus, lateral part
DRV	Dorsal raphe nucleus, ventral part
DTgP	Dorsal tegmental nucleus, pericentral part
DTT	Dorsal tenia tecta
EOV	Ependym of the olfactory ventricle

fmi	Forceps minor of the corpus callosum
FP	Frontal polar cortex
FPl	Frontal polar cortex, lateral part
FPm	Frontal polar cortex, medial part
Fr3	Frontal cortex, area 3
GI	Granular insula cortex
IF	Interfascicular nucleus
IL	Infralimbic cortex
IP	Interpeduncular nucleus
λ	Area lambda
LDTg	Laterodorsal tegmental nucleus
LO	Lateral orbital cortex
LHb	Lateral habenula
MHb	Medial habenula
lPFC	Lateral prefrontal cortex
mPFC	Medial prefrontal cortex
M1	Primary motor cortex
M2	Secondary motor cortex
MnR	Median raphe nucleus
MO	Medial orbital cortex
NeuN	Neuronal nuclear protein
oPFC	Orbital prefrontal cortex
PHA-L	*Phaseolus vulgaris*-leucoagglutinin
PBP	Parabrachial pigmented nucleus of the VTA
PFC	Prefrontal cortex
PMnR	Paramedian raphe nucleus
PN	Paranigral nucleus of the VTA

PrL	Prelimbic cortex
RLi	Rostral linear nucleus of the raphe
S1	Primary somatosensory cortex
SNC	Substantia nigra, pars compacta
SNR	Substantia nigra, reticular part
SMI-32	Neurofilament H marker SMI-32
VGLUT2	Vesicular glutamate transporter type 2
VGLUT3	Vesicular glutamate transporter type 3
VO	Ventral orbital cortex
VTA	Ventral tegmental area

TABLE 1 Primary antibodies used

Antigen	Immunogen	Source	Dilution	
			IPe	IF
5-HT	Serotonin coupled to bovine serum albumin (BSA) with paraformaldehyde	Immunostar, (Hudson, WI), #200800, rabbit polyclonal		1:40.000
CTb	Purified toxin from *Vibrio cholera*	List Laboratories, INC, (Burlingame, CA), #104, goat polyclonal	1:10.000	1:10.000
NeuN	Synthetic peptide of human NeuN	Biolegend, (San Diego, CA), #801701, mouse monoclonal		1:2.500
SMI-32	Non-phosphorylated mammalian neurofilament H	Abcam, (Cambridge, UK), #ab177487, rabbit monoclonal		1:2.500

Abbreviations: 5-HT, serotonin; CTb, cholera toxin, subunit b; NeuN, neuronal nuclear protein marker; SMI-32, neurofilament H; IF, immunofluorescence staining; IPe, immunoperoxidase staining.

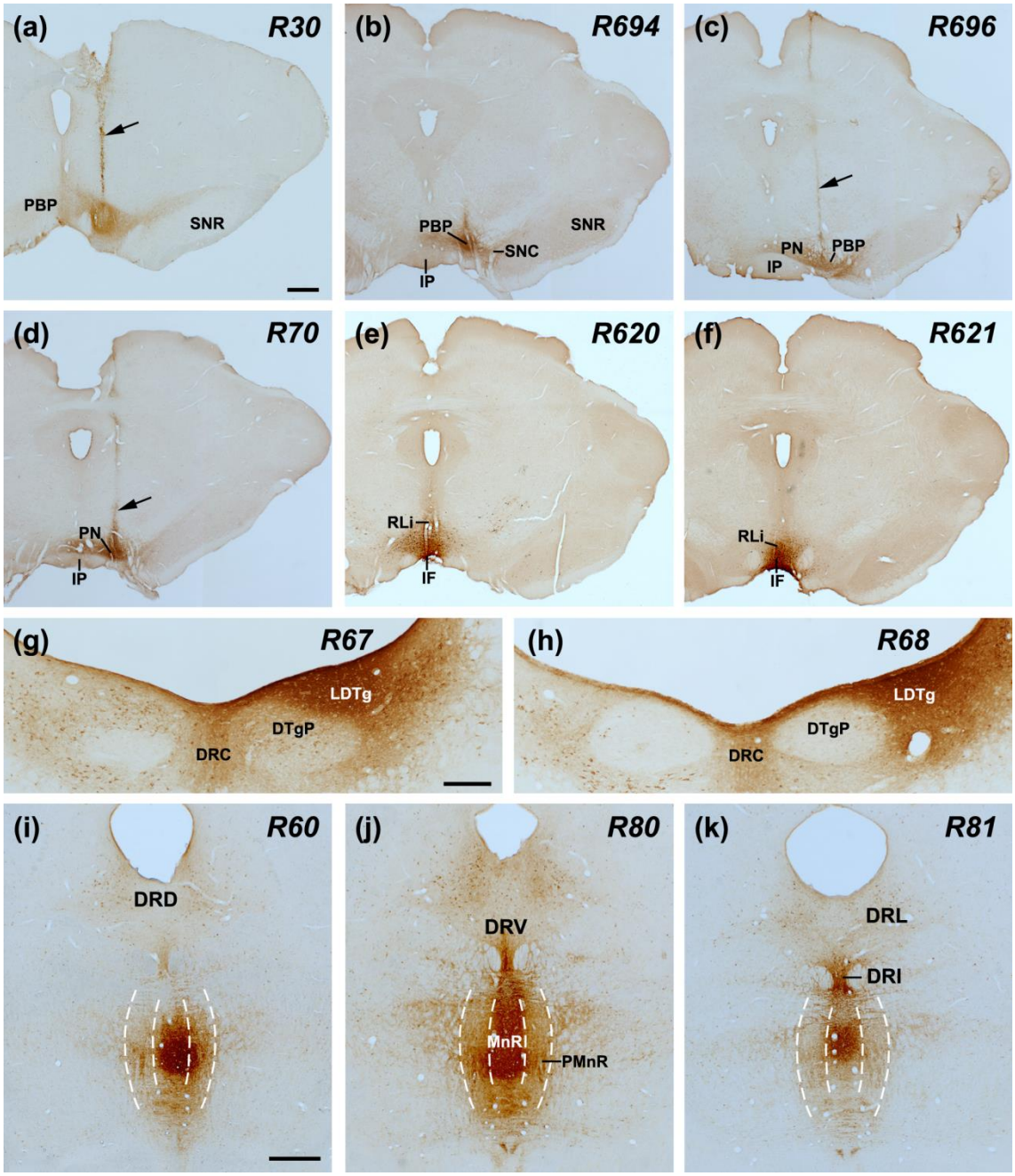

Fig. 1 CTb injection sites in the ventral tegmental area (VTA; (**a-f**), laterodorsal tegmental nucleus (LDTg; (**g, h**), and median raphe nucleus (MnR; (**i-k**). Case numbers are indicated in italics. The arrows point to the pipette tract. Scale bars = 500 µm in (a), (applies to a - f); 200 µm in (g), (applies to g - h); 400 µm in (i), (applies to i – k)

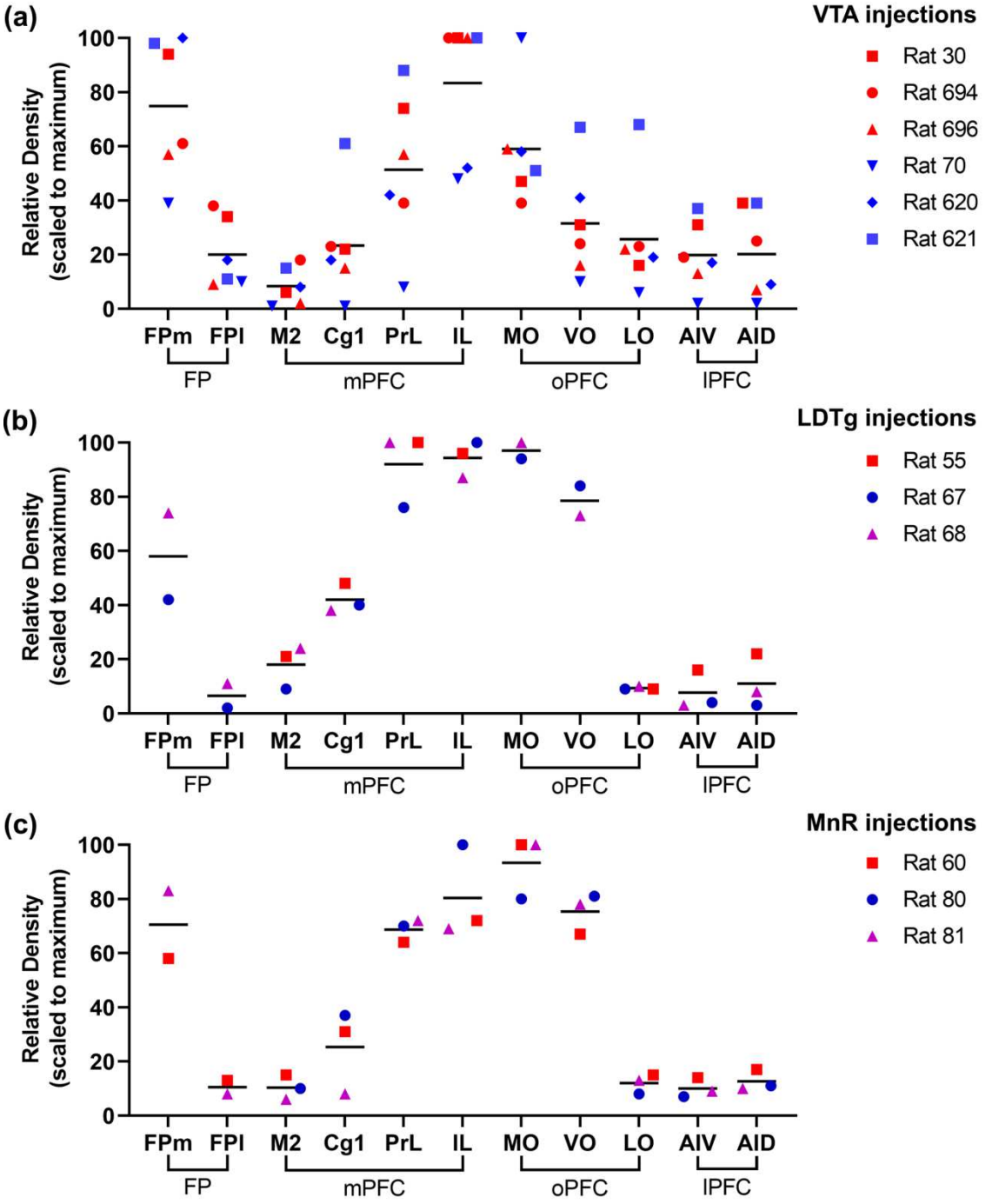

Fig. 2 Histograms of the relative densities of labeled cells in prefrontal cortical areas following injection of CTb into: (a) the VTA; (b) the LDTg; (c) the MnR. Each density value was scaled relative to the maximum within that brain. The labeled cells were counted at specific levels, illustrated in Figures 4-6, 8, and 10. Counting in FPm/FPl was performed at level (a); in MO at level (b); in VO at levels (b, c); in Cg1, LO, M2, PrL, and AID/AIV at levels (b - f), and in IL in levels (c – f). Please note that levels (a, b) in case R55 and level (a) in case R80 were not available.

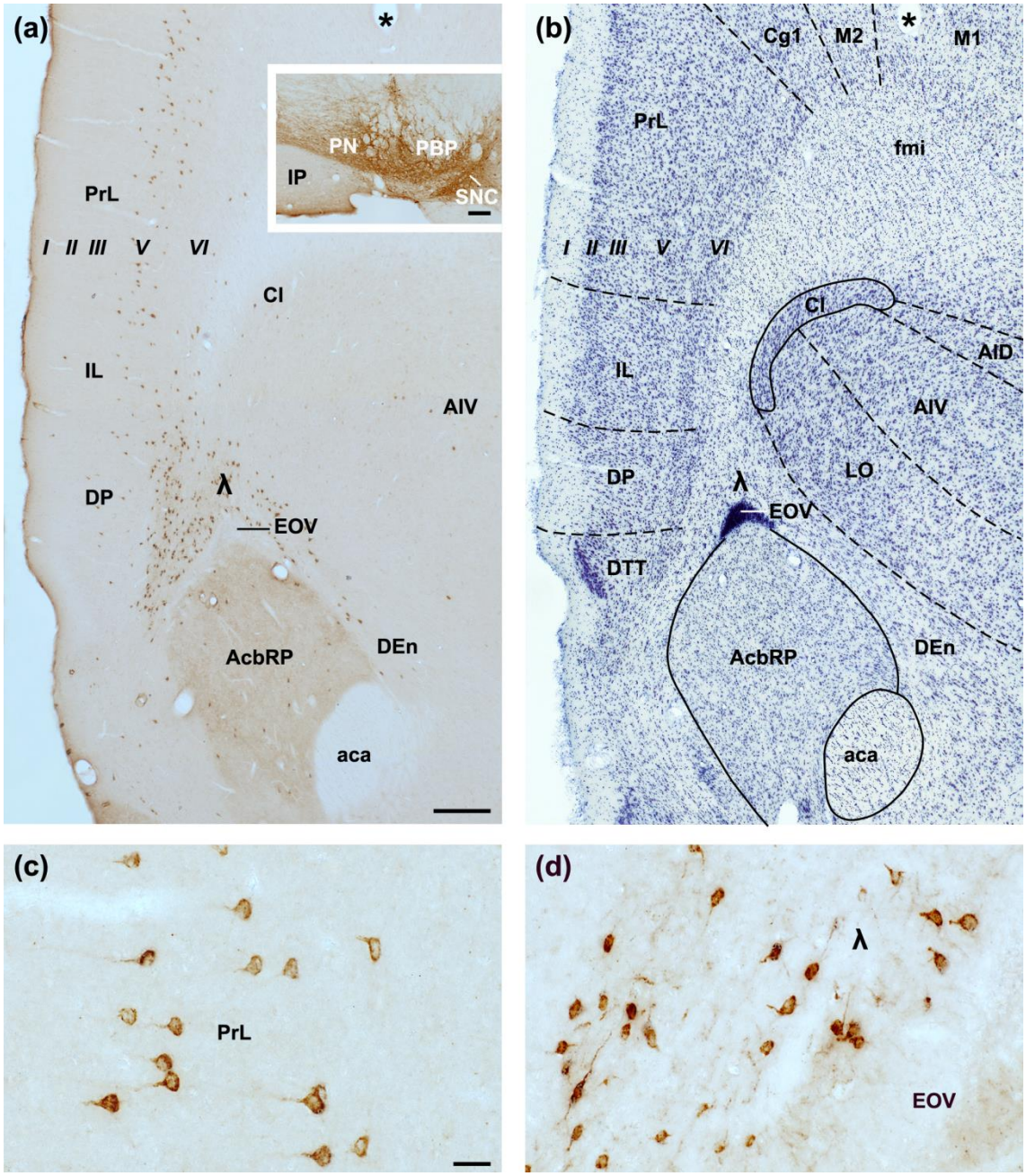

Fig. 3 (a) Low-power photomicrographs of retrograde labeling in the ventromedial PFC resulting from a CTb injection into VTA in case R696 (inset, Fig. 1c) and an adjacent Nissl stained section (b). High-power micrographs of CTb-labeled neurons in the ventral prelimbic (PrL) cortex (c), and an area overlying the apex of the rostral pole of the nucleus accumbens (AcbRP) here tentatively named area λ (d). Note that most cortical CTb+ neurons are confined to cortical layer V and show morphological characteristics of pyramidal neurons (c), whereas CTb+ neurons in area λ display characteristics of polymorph neurons (d). Asterisks indicate the same blood vessel in (a) and (b). Scale bar = 500 µm in (a), (applies to a, b); 100 µm in the inset, 20 µm in (c), (applies also to d)

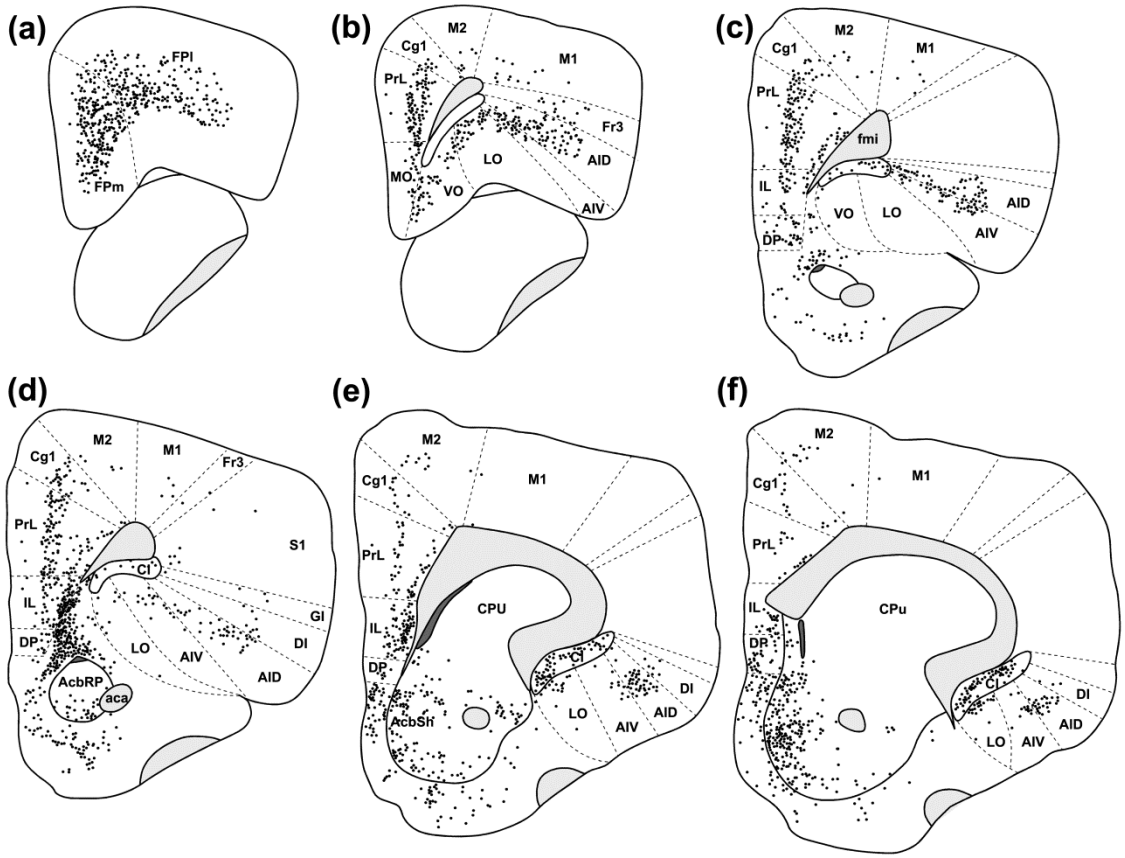

Fig. 4 Schematic representations of retrogradely labeled neurons at six consecutive rostrocaudal levels through the PFC. CTb labeling stems from the CTb injection (case R30) centered on the parabrachial subnucleus (PBP) of the VTA depicted in Figure 1a. Each retrogradely labeled neuron is represented by one dot. Note that most of the CTb+ neurons are found in deep cortical layers V and VI.

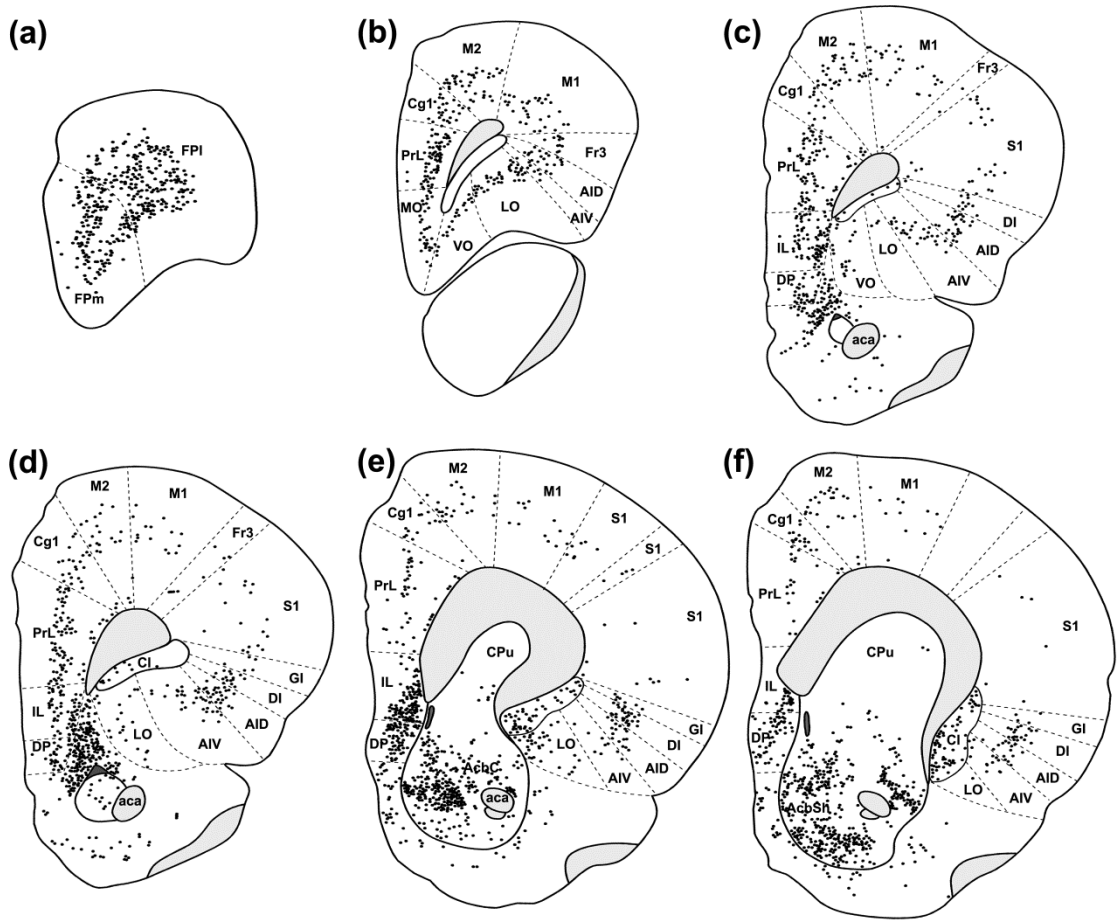

Fig. 5 Schematic representations of retrogradely labeled neurons at six consecutive rostrocaudal levels through the PFC. CTb labeling stems from the CTb injection (case R694) centered on the lateral part of PBP and involving peripherally the SNC, depicted in Figure 1b. Each retrogradely labeled neuron is represented by one dot. Note the substantial number of CTb+ neurons in the primary motor (M1) and sensory (S1) cortex. Note also the additional labeling in the accumbens core (AcbC) and ventrolateral caudate putamen (CPu).

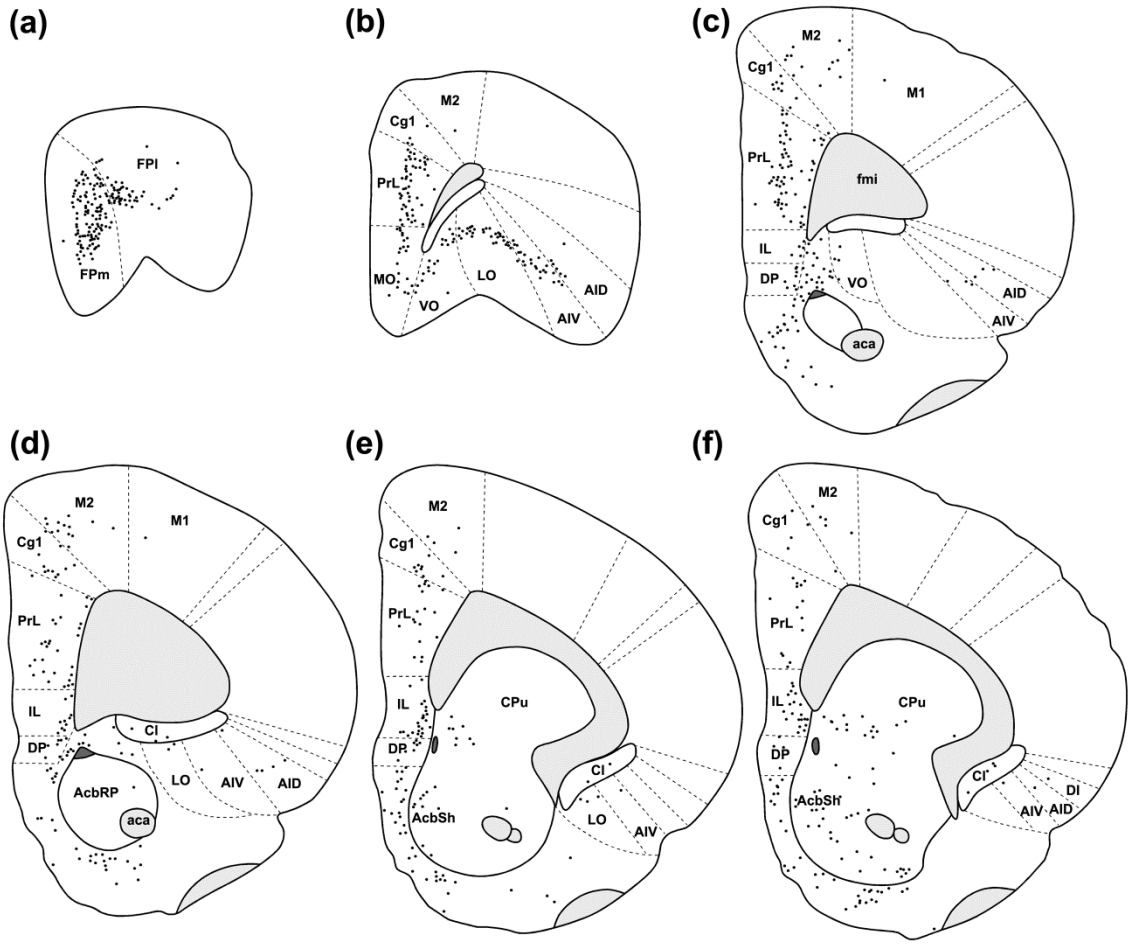

Fig. 6 Schematic representations of retrogradely labeled neurons at six consecutive rostrocaudal levels through the PFC. CTb labeling stems from the CTb injection (case R620) centered on the midline VTA interfascicular (IF) and rostral linear (RLi) VTA subnuclei depicted in Figure 1e. Each retrogradely labeled neuron is represented by one dot.

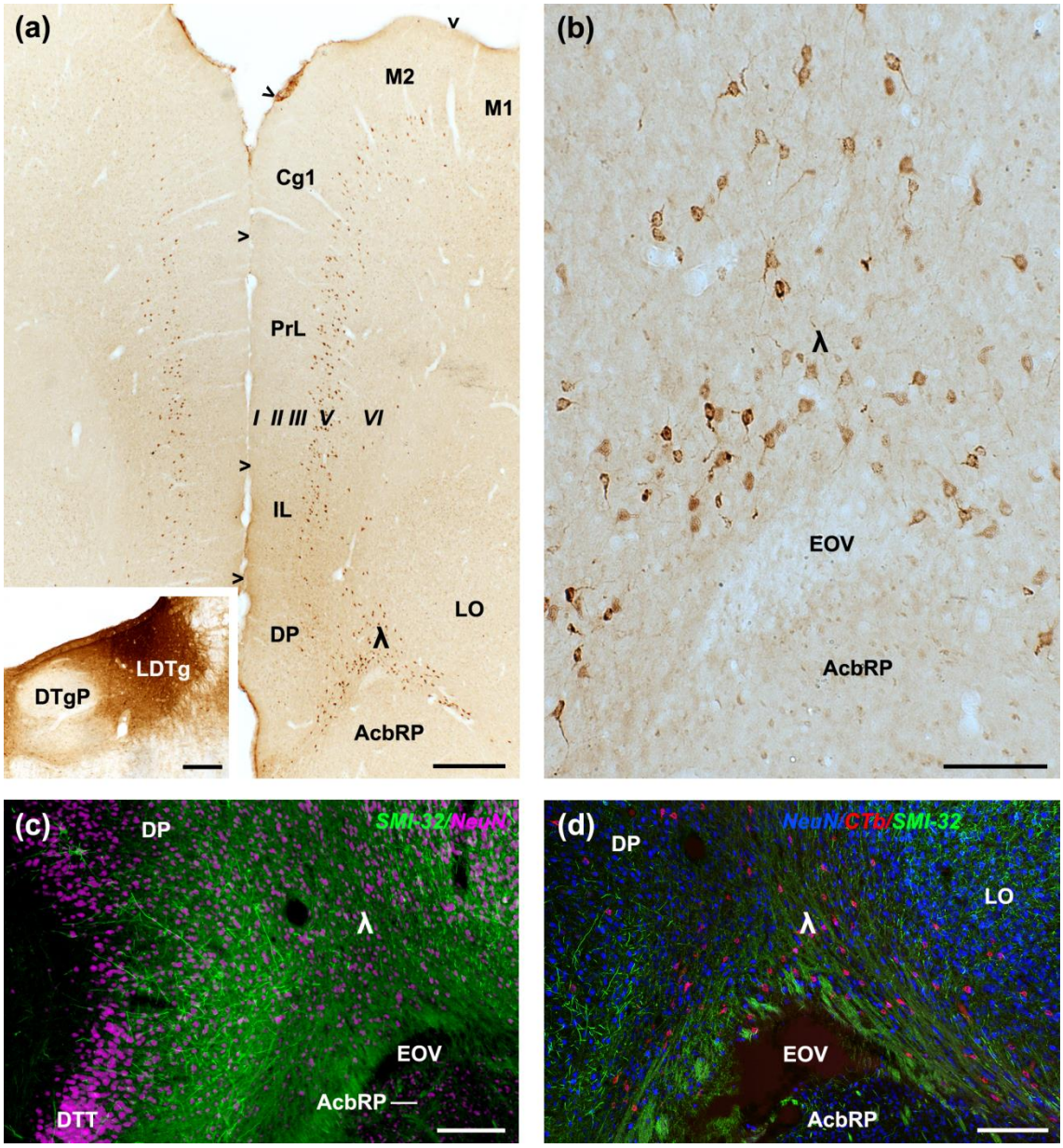

Fig. 7 (**a**) Low-power photomicrographs of bilateral retrograde labeling in the medial PFC resulting from a CTb injection into LDTg in case R55 (inset). (b) High-power photograph of CTb+ neurons in area λ. Note the non-pyramidal morphology of most of these neurons (c) Double immunofluorescence staining for the neuronal nuclear protein marker NeuN and the neurofilament protein marker SMI-32 in area λ and adjacent deep peduncular (DP) cortex. (d) Confocal image of triple immunofluorescence staining for CTb/SMI-32/NeuN in area λ and adjacent DP and lateral orbital (LO) cortex of case R55. Note that most of the CTb+ neurons overlying the apex of the AcbRP are found nestled between SMI-32+ bundles in area λ. Scale bar = 250 µm in (a); 200 µm in the inset, 100 µm in (b), (c), (d)

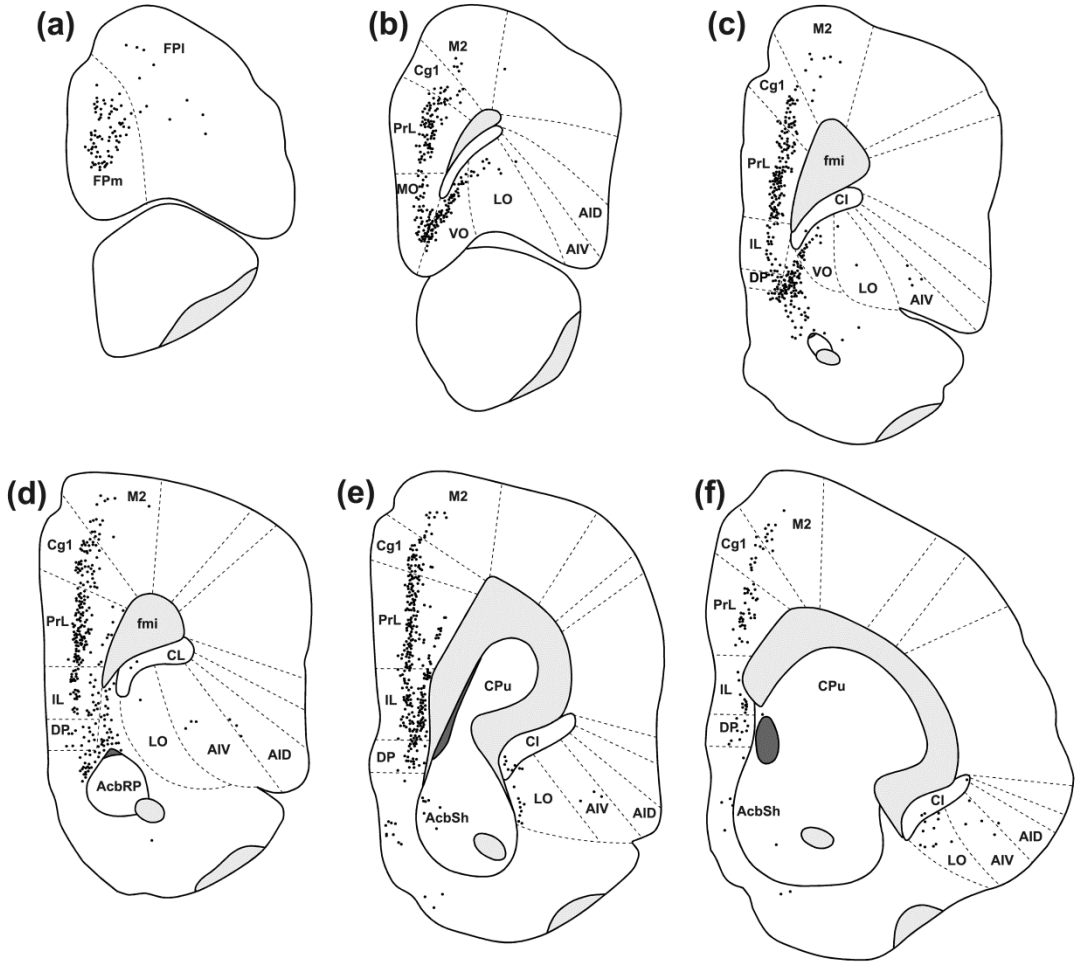

Fig. 8 Schematic representations of retrogradely labeled neurons at six consecutive rostrocaudal levels through the PFC. CTb labeling stems from the CTb injection (case R67) centered in the dorsal part of the LDTg depicted in Figure 1g. Each retrogradely labeled neuron is represented by one dot.

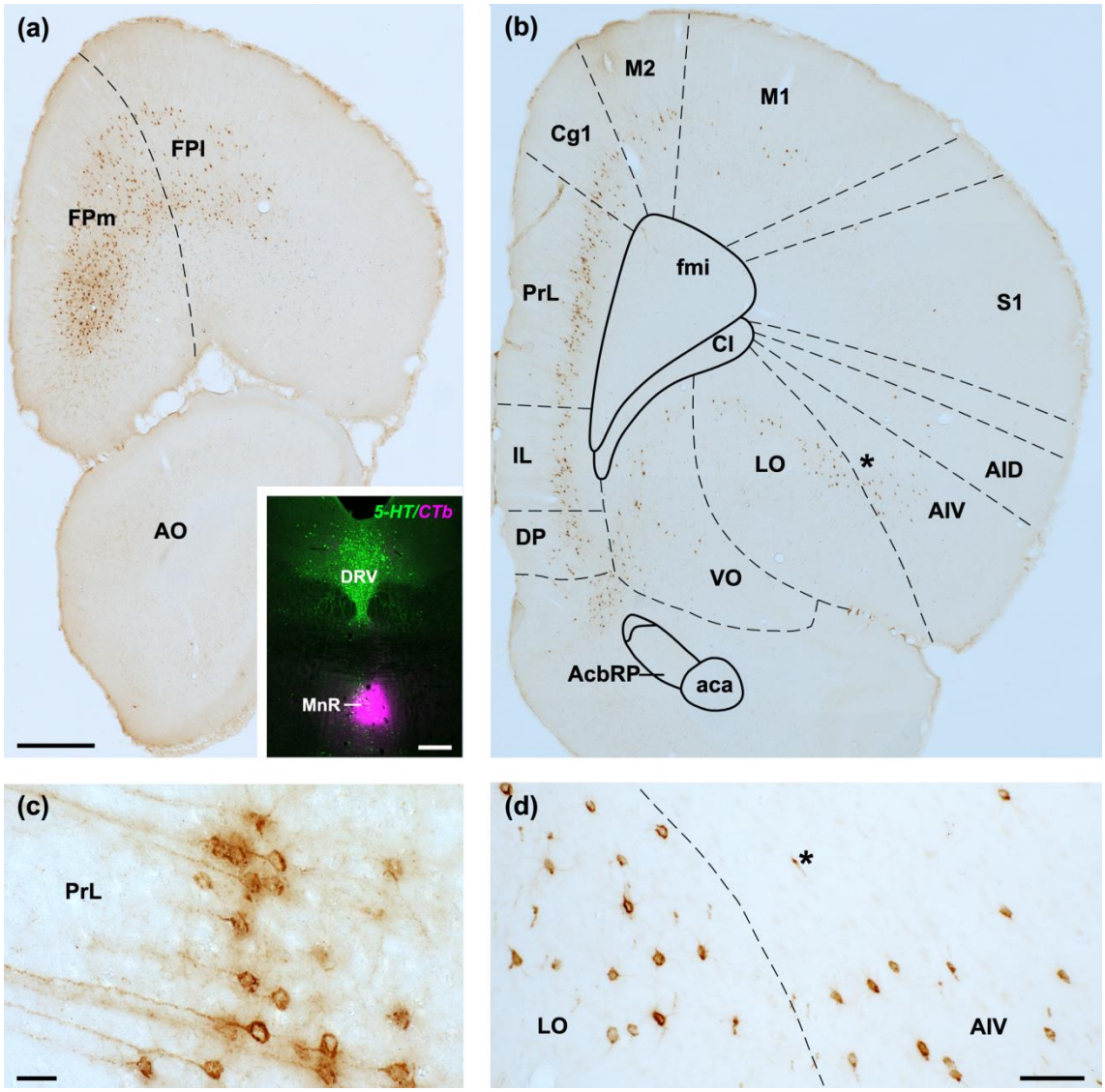

Fig. 9 Low-power photomicrographs of retrograde labeling resulting from a CTb injection into MnR in case R60 (inset, see also Fig. 1i) at a rostral (**a**) and midrostrocaudal (**b**) level through the PFC. CTb+ neurons in the prelimbic (PrL) cortex (**c**) and at the border between the lateral (LO) and ventral agranular insular (AIV) cortex (**d**). Note the different morphology of CTb+ neurons in LO and AIV. Asterisks indicate the same blood vessel in **b** and **d**. Scale bar = 500 µm in (a), (applies also to b); 20 µm in (c); 100 µm in (d)

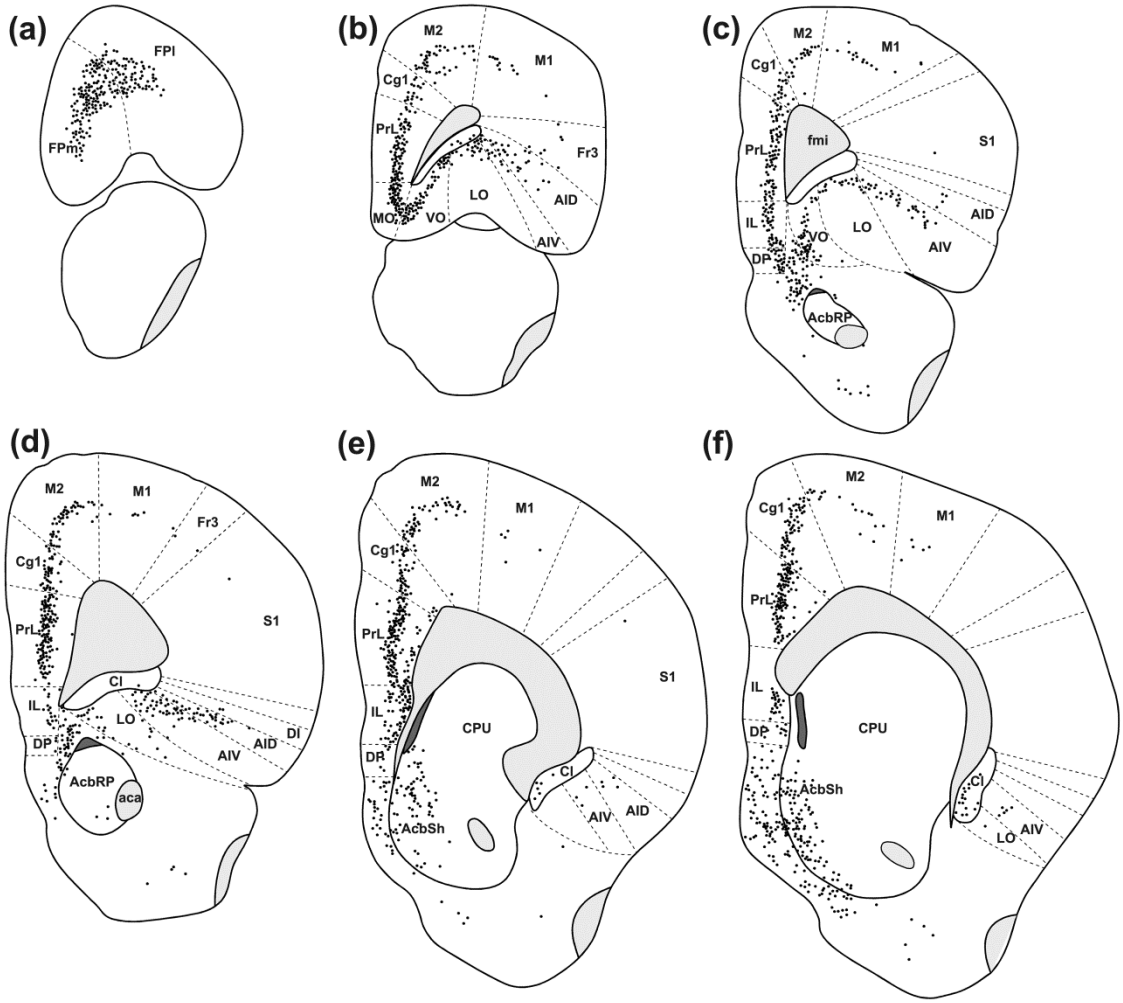

Fig. 10 Schematic representations of retrogradely labeled neurons at six consecutive rostrocaudal levels through the PFC. CTb labeling stems from the CTb injection (case R60) filling most of the MnR/PMnR depicted in Figure 1i. Each retrogradely labeled neuron is represented by one dot.

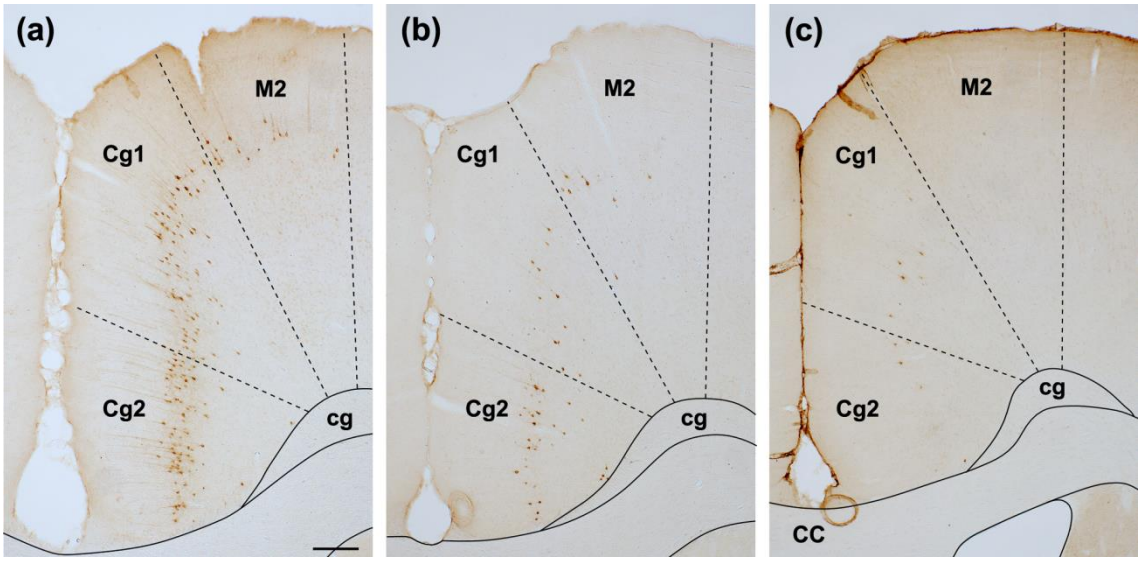

Fig. 11 Low-power photomicrographs of retrograde labeling in the cingulate areas 1 (Cg1) and 2 (Cg2), as well as in the secondary motor cortex (M2) resulting from CTb injections into the MnR (case R60, **a**), LDTg (case R55, **b**), or VTA (case R696, **c**), respectively. Note in (**a**) the more substantial retrograde labeling following tracer injections into MnR. Scale bar = 200 µm in (a), (applies to a - c)

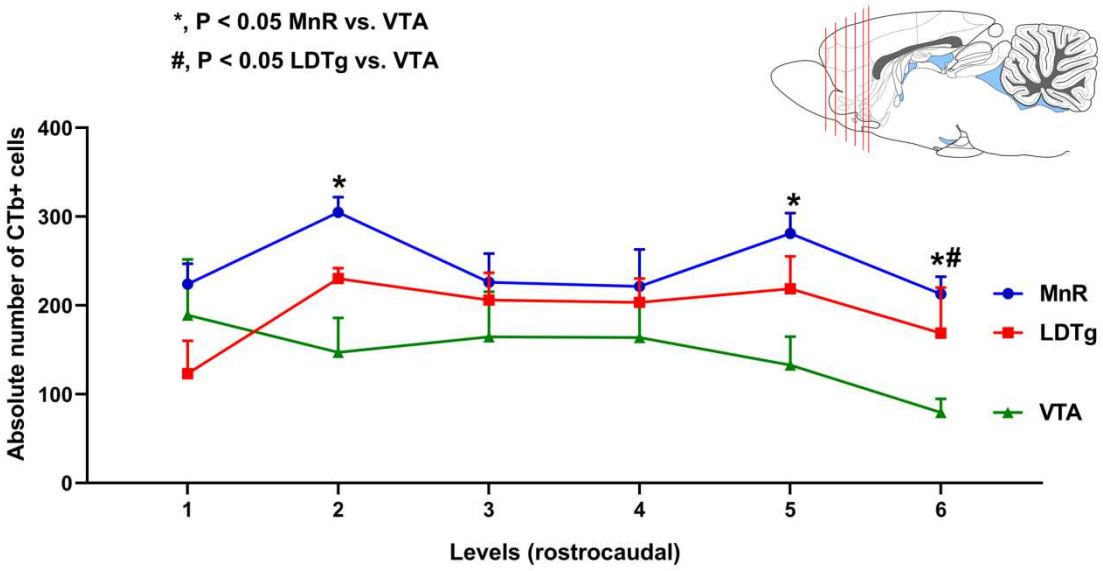

Fig. 12 Graphs depicting absolute numbers of VTA- (sample size = 5258, n = 6), LDTg- (sample size = 3327, n = 3), and MnR- (sample size n = 4185, n = 3) projecting neurons at six PFC levels along the rostrocaudal axis of the brain (indicated in the inset). Shown are means ± SEM of numbers of retrogradely labeled neurons per brain section on the ipsilateral side in rats injected into the MnR (blue circles), LDTg (red squares), and VTA (green triangles). * $P < 0.05$ MnR versus VTA. # $P < 0.05$ LDTg versus VTA (one-way ANOVA and Newman-Keuls multiple comparisons test).

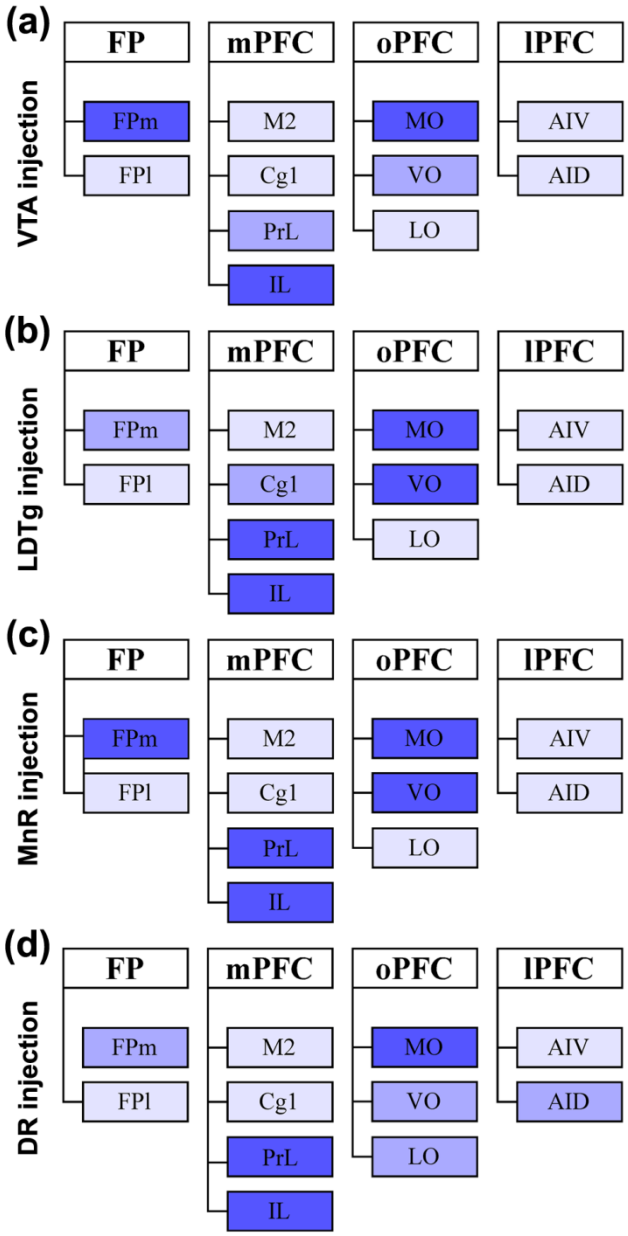

Fig. 13 Schematic diagram summarizing the relative densities of afferents emerging from distinct PFC subfields to the VTA (a), LDTg (b), and MnR (c). Dark blue filling of rectangles indicates high densities, lilac filling medium densities, and light blue filling low densities of afferents originating from this PFC subregion, respectively. For abbreviations, see list. In (d) we also included summarized findings from a previous study of our group (Gonçalves et al. 2009), in which we investigated by the same methodology applied here prefrontal afferents to the dorsal raphe nucleus (DR).